Macromolecules

Article

Cite This: *Macromolecules* 2018, 51, 7924−7941

pubs.acs.org/Macromolecules

Connecting Pressure-Dependent Dynamics to Dynamics under Confinement: The Cooperative Free Volume Model Applied to Poly(4-chlorostyrene) Bulk and Thin Films

Ronald P. White and Jane E. G. Lipson*

Department of Chemistry, Dartmouth College, Hanover, New Hampshire 03755, United States

ABSTRACT: We apply our cooperative free volume (CFV) rate model for pressure-dependent dynamics to describe the relaxation times for poly(4-chlorostyrene) (P4ClS) bulk and thin films. The CFV model expresses segmental relaxation times, τ, as a function of temperature, T, and thermodynamic free volume, $V_{free} = V - V_{hc}$, where the limiting hard core volume, V_{hc}, is obtained via analysis of a polymer's experimental PVT data using the locally correlated lattice (LCL) model equation of state. In adapting CFV to describe thin films, we assume that the main effect of confinement is that the interface serves to change the average free volume (average density) compared to bulk. We formulate a simple weighted average expression (involving just a single interface related parameter) to describe the free volume of a film as a function of thickness, h, and use this h-dependent V_{free} within the CFV model expression. Using just ambient pressure relaxation time data on bulk P4ClS, along with PVT data, we parametrize the CFV model, which is then able to predict both the P-dependent dynamics for the P4ClS bulk and the thickness-dependent dynamics of P4ClS films; the CFV parameters are transferable for either scenario. Analysis of the bulk P-dependent dynamics predictions for P4ClS indicates a strong sensitivity to volume changes, and this leads to a strong sensitivity to confinement (h). In addition, we show that the effect of confinement, e.g., for a 15 nm P4ClS film, is analogous to the effect of a P decrease on the order of about 25 MPa or so. The model τ vs h behavior is in close agreement with the form of the isothermal experimental data. Furthermore, we show predictions for the film behavior at other temperatures, based on analysis of the limited (T = 433 K) experimental data that are available.

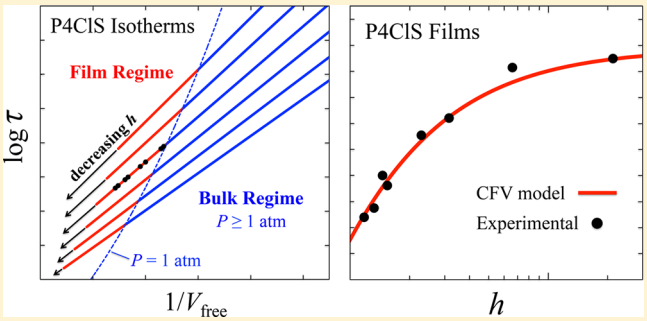

1. INTRODUCTION

An ongoing challenge in the study of polymer melts and other glass-forming liquids is to gain a deeper understanding of their dynamic properties.[1−18] Examples include structural/segmental relaxation times (τ), viscosity (η), diffusion (D), and other transport quantities as well as the system's glass transition temperature (T_g). An approach that has the potential to provide mechanistic insight is to study "pressure (P)-dependent dynamics",[1,3] which focuses on the system's response to independent changes in temperature (T) and volume (V). We have recently developed the cooperative free volume (CFV) model, in which thermodynamic characterization of a system over PVT space leads to a prediction for the T- and P-dependent free volume (V_{free}). We have found V_{free} to be a natural variable for understanding dynamic relaxation along with a system-dependent temperature contribution.[19−21]

In this work we use the CFV model to show how the ability to describe pressure-dependent dynamics for a bulk system advances the understanding of that system's dynamics under confinement. Our results for polymer films are particularly timely in light of the recent studies of Adrjanowicz et al.[22,23] and Tarnacka et al.[24] on small molecules confined in nanopores, where they demonstrated that a system's confined dynamics can be mapped into a connection with its general P-dependent bulk behavior.

The presence of interfaces in confined glass-forming systems (i.e., in films (1D), nanopores (2D), nanospheres (3D), etc.) leads to diverse changes in their dynamics compared to bulk.[6,25−29] One way of thinking about the effect of varying the degree of confinement (e.g., by varying polymer film thickness, h) is that it allows the system to visit points in T, V space that would not be accessible to the bulk at ambient pressure. An essential goal of this work, therefore, is to model how a system responds to *independent* changes in temperature and volume.

At a small distance from the interface of a liquid, e.g., near an equilibrium free surface at some T, P, there may be a change in local density compared to the interior of the bulk.[30−32] (See the Appendix for a detailed picture.) While the effect on a finite system's sample-averaged density may seem small, the relative local impact on free volume (V_{free}) may be sufficient to alter local segmental motion, thus leading to a significant effect on the dynamics.

Received: June 29, 2018
Revised: August 15, 2018
Published: October 1, 2018

DOI: 10.1021/acs.macromol.8b01392
Macromolecules 2018, 51, 7924−7941

Another important category of interface-related density changes arises from nonequilibrium (or quasi-equilibrium) conditions. Napolitano and co-workers[33−35] have shown that supported polymer films, prior to annealing, can have an excess of free volume at the polymer−substrate interface. Measurements for polystyrene (PS) on Al[33] showed that this extra space then allowed for (irreversible) probe adsorption onto the substrate, to a degree which depended on the degree of prior annealing. The authors found that as annealing time increased the gradual "filling in" of the extra free space in the interfacial region led to a gradual recovery of the bulk relaxation times. A similar effect of density equilibration on the dynamics of polymers in nanopores (via annealing) has recently been demonstrated in Tarnacka et al.[36]

In this work we extend our CFV model expression for $\tau(T,V_{free})$ of bulk systems[19−21] to the case of confined samples; the key change is to take V_{free} to reflect a *sample-averaged* free volume. We express the film-averaged V_{free} as a simple function of its thickness, h, leading to a result for $\tau(T,h)$ in which segmental relaxation times are described as a function of T and h for films at ambient pressure. An important step is to assume that the CFV model's system-dependent parameters are *transferable* from the bulk to the film environment. This simplification means that only a single, new, interface-related parameter appears.

We then apply this model to analyze experimental segmental relaxation time results on poly(4-chlorostyrene) (P4ClS) films obtained by Panagopoulou and Napolitano using dielectric spectroscopy.[35] These particular P4ClS films are capped by Al layers, and the data that we model here concern results before any annealing (t_{ANN} = 0; before the chains become strongly adsorbed). Here the confining interface (Al substrate) serves as a repulsive/nonattractive boundary, playing a role similar to that of a free surface, such that there is an excess of free volume available, and this leads to a lower sample average density.

An outline of the remainder of the article is as follows. Section 2 covers background, including details of the cooperative free volume model for bulk systems. In section 3, the bulk $\tau(T,V_{free})$ expression is then extended to describe $\tau(T,h)$ for film applications. In section 4, we use the bulk model to predict the pressure-dependent dynamics of P4ClS using only ambient dynamics data as input. We demonstrate the effectiveness of this predictive route using PVAc as an illustrative example. In section 5 we predict the free volume values for P4ClS films and plot the T, V_{free} dynamics space for P4ClS in the form of a generalized map connecting the bulk regime with the confined system (film) regime. Using our V_{free} predictions, we then apply the CFV $\tau(T,h)$ expression to describe dynamic relaxation in P4ClS films and compare with the limited experimental data available. In section 6, we provide a summary.

2. THE CFV MODEL AND THE ROLE OF FREE VOLUME IN PRESSURE-DEPENDENT DYNAMICS

2.1. Basic Considerations and Key Equations. Modeling the pressure-dependent dynamics of glass-forming liquids, i.e., to express $\tau(T,V)$, is a challenging problem. Even on an isobar the Arrhenius form, $\tau = A\exp[B/T]$, does not work well, nor does the simple volume dependence of the Doolittle equation,[37] $\tau = A\exp[B/V_{free}]$. The phenomenological VFT expression,[38−40] $\tau = A\exp[B/(T - T_0)]$, with a third parameter, T_0, can fit the dynamics where T changes along a single thermodynamic path; however, it does little to explain the behavior. A single set of VFT parameters is only applicable to a single isobar or isochore, so it cannot describe P-dependent dynamics.

We have found that a system's free volume, V_{free}, appears to be strongly connected to its dynamic relaxation. For instance, we have shown[19−21] for a number of experimental and simulated systems that whenever T is fixed (i.e., on an isotherm), a plot of ln τ vs $1/V_{free}$ produces a linear relationship, with each line (isotherm) having a T-dependent slope. A key point is that our free volume predictions are calculated independently of dynamics data, being based on analysis of pressure−volume−temperature (PVT) data. Our definition is physical and straightforward: V_{free} is the difference between a system's overall volume, V, and its limiting, closely packed, hard-core value, V_{hc}.

$$V_{free} = V - V_{hc} \tag{1}$$

V_{hc} is a constant for each system, independent of both T and P, its value being determined as part of our analysis of the PVT surface. In addition to our independent route for V_{free} values, an essential difference between our approach and historical (Doolittle equation-based) free volume models[41−43] is that while the CFV model incorporates V_{free} as a *natural* variable, determining the volume contribution to dynamics, it is not the only variable; an independent functional dependence on T is also required.

There are other routes to quantifying free volume in the literature.[44] For example, some conceptualize separate "vibrational" and "excess" contributions. Another popular measure is the Debye−Waller factor, which is strongly connected to dynamic relaxation,[45−51] although the fact that it can still change with T at constant volume means that it differs considerably from our V_{free}. As eq 1 shows, V_{free} will only change when there is a change in volume.

The CFV model shares some similarities with the well-known model of Adam and Gibbs (AG).[52] Both involve rate expressions wherein the activation energy (ΔA_{act}) depends on the number of nearby segments needed to cooperate so as to allow a segmental rearrangement. The AG model quantifies this number (z^*) of segments based on configurational entropy (S_c), obtaining $z^* \propto 1/S_c$, leading to the AG form $\ln \tau \sim [\text{constant}]/TS_c$. By comparison, in the CFV model, the number (n^*) of cooperating segments is quantified by free volume, such that we obtain $\Delta A_{act} \propto n^* \propto 1/V_{free}$ as the key relationship that controls the volume dependence of the model activation free energy. A mechanistic derivation of the CFV model is described in the next subsection. An overview of the main equation(s) and context on some of the advantages of the approach is provided here.

We apply the CFV model to pressure-dependent dynamics in one of two related forms, depending on the temperature range of application. Both forms have the same volume dependence ($\sim 1/V_{free}$) and differ only in T dependence. They both can be derived starting from the same CFV model framework, up to the point that produces the expression $(1/V_{free}) \times f(T)$, which is a mechanistic consequence of the free-volume-based cooperativity.[20] One form follows from a very simple assumption of constant energy and entropy of activation per cooperating segment and is given by

$$\ln \tau = C_1\left(\frac{V_{hc}}{V_{free}}\right)\left(1 + \frac{C_2}{T}\right) - \ln T^{1/2} + C_3 \tag{2}$$

DOI: 10.1021/acs.macromol.8b01392
Macromolecules 2018, 51, 7924−7941

Comparison with simulation data has shown that eq 2 is correct over a wide range of pressure-dependent conditions at high T, including the Arrhenius to non-Arrhenius crossover regime. It has yielded fundamental insight, e.g., explaining the volume contribution to non-Arrhenius behavior on isobars.[20,21] At low temperature its T dependence is not strong enough, though the volume dependence remains correct.

The other CFV form has a T dependence that is appropriate at lower T, in the range of T from T_g up to about $1.4T_g$ or so, which is the typical glassy dynamics range probed in dielectric spectroscopy experiments. This will be the form applied here and is given by

$$\ln \tau = \left(\frac{V_{hc}}{V_{free}}\right)\left(\frac{T^*}{T}\right)^b + \ln \tau_{ref} \tag{3}$$

Note the gas kinetic $\ln T^{1/2}$ term is not required at low T,[20] and the notation for the parameters (b, T^*, τ_{ref}) comes from our original article.[19] The T dependence in eq 3 is empirical; the overall form adheres to the $(1/V_{free}) \times f(T)$ cooperative mechanistic structure.

There are experimental results supporting the notion that cooperativity is based on free volume. For example, Hong et al.[53] studied the cooperativity (heterogeneity) length scale from boson peak spectra for a large number of glass-forming systems and found a strong correlation with a system's activation volume for segmental dynamics. They could not discern a correlation between cooperativity and system fragility (T dependence) and suggested that only the volume dependence of segmental dynamics correlates with the size scale of cooperativity. Consistent with their results, we have shown, at least for the high-T regime, that (free) volume is indeed the only source of cooperativity and non-Arrhenius behavior.[20,21]

One of the advantages of CFV over other approaches, such as pressure-dependent implementations of the AG model,[54−57] is that free volume is a more straightforward quantity to define, evaluate, and apply compared to pressure-dependent configurational entropy. Another is that the CFV method requires fewer parameters to be determined through analysis of the dynamics data it is trying to capture. It is typical that models for pressure-dependent dynamics involve about four parameters. The often-applied $\ln \tau = (C/TV^\gamma)^\phi + \ln \tau_0$ expression developed in Casalini et al.[58,59] is a good benchmark example; the AG-based approaches[54−57] usually have four or five. The CFV description is more efficient because all systems follow the same natural form of volume dependence, going as $1/V_{free}$, and in applying the model equation, V_{hc} is not determined from the dynamics data, but instead from analysis of the system's thermodynamic properties. This leaves only three "dynamics parameters", which therefore require less data to specify; thus, the model is able to make predictions about relaxation over a broader temperature and pressure range than experimental results may cover.

2.2. Details of the CFV Rate Model. In this subsection we derive eq 3 via the cooperative free volume rate model framework, providing a more mechanistic explanation than we gave in our original application to experimental systems.[19]

In a liquid system of N total particles (segments), consider the amount of time it takes for a particle (segment) to move out of the "cage" of its surrounding neighbors, i.e., to travel a distance on the order of its own size. This requires a number, n^*, of nearby particles to redistribute in such a way that some necessary amount of free volume, v^*, is gathered on site, thus creating the new space into which the particle can move. When this amount of consolidated free space has been created, the cooperating particles are in what we call the "activated state". The probability for forming the activated state is denoted by P_{act} and is formulated further below.

Figure 1 is a schematic illustration of how the cooperative space-opening process might work. As the free volume in the system decreases, more particles (segments) must operate together to open up the required amount of free space (i.e., n^* will increase). Because a characteristic-sized opening is required to fit a segment, we assume a cooperating group must have in total a characteristic amount of free volume (v^*) to make that space. From this, it follows that

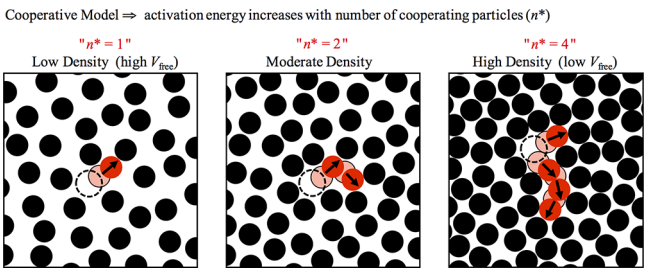

Figure 1. Schematic showing cooperating particles (red), before they make their moves (semitransparent red), and then after (solid red); remaining liquid particles are black. After the moves are made, the resulting configuration corresponds to the "activated state" where a full particle-sized vacancy has been created (dashed circle), and once this is formed (or concurrently with its formation), another particle can move into the vacancy to make a full diameter-scale translation and thus escape its previous cage of neighboring particles. As density increases (V_{free} decreases), the number of cooperating particles must increase to make the same-sized vacancy; in this example n^* increases from 1 to 2 to 4. The CFV model activation free energy depends on n^*: the higher the n^*, the lower the probability of the activated state. Reproduced with permission from ref 21.

$$n^* = v^*/(V_{free}/N) \tag{4}$$

The number of cooperating particles, n^*, is inversely proportional to the average free volume per particle, and this is a key link in explaining why $1/V_{free}$ is the natural variable for describing the volume contribution to dynamics.

A central quantity in describing the segmental relaxation rate is P_{act}, the probability of the activated state, which depends on the associated activation free energy, ΔA_{act}. Here we expect ΔA_{act} to increase with the number of cooperating particles (n^*), which is also a feature of the entropy-based model of Adam and Gibbs. We define $\Delta A_{act} = n^* \Delta a$, where ΔA_{act} is the *total* Helmholtz free energy change for the n^* particles to go into their activated state (i.e., to form a space), while $\Delta a = \Delta A_{act}/n^*$ is the activation free energy per cooperating particle. The probability of the activated state is therefore

$$P_{act} = \exp[-\Delta A_{act}/T] = \exp[-n^* \Delta a/T] \tag{5}$$

This form fundamentally reflects the cooperative structure of the model. (The Boltzmann constant has been absorbed for simplicity.) Using $n^* = v^*/(V_{free}/N)$ inside eq 5, P_{act} then becomes

$$P_{act} = \exp\left[-\left(\frac{v^*}{(V_{free}/N)}\right)\left(\frac{\Delta a}{T}\right)\right] \tag{6}$$

DOI: 10.1021/acs.macromol.8b01392
Macromolecules 2018, 51, 7924−7941

The relaxation rate, R, is expected to have a general form, R = [constant] × $T^{1/2}$ × P_{act}. Here we ignore the gas kinetic T dependence (average velocity going as $T^{1/2}$) and simply take $R \propto P_{act}$. This is acceptable for modeling most dielectric spectroscopy data because in that range of application the exponential should dominate (see ref 20). The relaxation time $\tau \propto 1/R \propto 1/P_{act}$ is written as

$$\ln \tau = \left(\frac{V_{hc}}{V_{free}}\right)\left(\frac{N\nu^*\Delta a}{V_{hc}T}\right) + \ln \tau_{ref} = \left(\frac{V_{hc}}{V_{free}}\right) f(T) + \ln \tau_{ref} \quad (7)$$

where the additive constant, ln τ_{ref}, arises from the multiplicative constant in $\tau \propto 1/P_{act}$ and where the (dimensionless) relative free volume, V_{free}/V_{hc}, is used. In the high-T regime, which includes the non-Arrhenius crossover region, we have shown[20] that ν^* is indeed a constant, independent of both T and V, and that $\Delta a/T \propto (1 + C/T)$ follows from simple assumptions; this leads directly to eq 2. However, in the more strongly super-Arrhenius low-T regime, the product, $\Delta a\nu^*$, develops a T-dependence (in Δa and/or ν^*) that we cannot formally derive. The experimental results of Hong et al.[53] do not rule out the possibility that ν^* remains T independent, with the unknown T dependence being carried by Δa. In any case, the assumption that Δa and ν^* are always *volume independent* does still hold, and so they can be absorbed into the combined quantities comprising $f(T)$, a function of T only.

Equation 7 is a fundamental result that follows from the model's V_{free}-based cooperativity relationship, $\Delta A_{act} \propto n^* \propto 1/V_{free}$. The $(V_{hc}/V_{free}) \times f(T)$ product form *predicts* that on isotherms ln τ will depend linearly on inverse free volume, and these lines will have T-dependent slopes. An example of this behavior is shown for PVAc relaxation times[60,61] in Figure 2.

The structure of eq 7 is enough to deduce an empirical T dependence applicable for the low-T regime. With the correct $f(T)$, it follows that a plot of ln τ vs $(1/V_{free}) \times f(T)$ should produce a single line that accounts for all pressure-dependent T, V_{free} points. This is the route we followed in deducing the form for $f(T)$ in ref 19. In analogy to other thermodynamic scaling approaches,[1,3,50,58,59,62−69] we applied a scaling exponent, b, in this case to the temperature, since the functional dependence on V_{free} (as described above) was clearly successful. With the correct choice of b, plots of ln τ as a function of $1/(T^bV_{free})$ collapsed neatly into linear form for all experimental systems we tried. The inset of Figure 2 shows an example. The slope and intercept of the collapsed line lead directly to the two remaining system-dependent parameters. Therefore, using the approximate $f(T) = (T^*/T)^b$ in eq 7, we thus arrive at eq 3, ln $\tau = (V_{hc}/V_{free})(T^*/T)^b$ + ln τ_{ref}, with parameters, b, T^*, and τ_{ref}. Note that only one of the three, b, has been optimized.

3. CFV MODEL FOR DYNAMICS UNDER CONFINEMENT

To model a polymer film, we start with the eq 3 $\tau(T,V_{free})$ expression for bulk P-dependent dynamics. We assume that the effect of varying film thickness (h) is manifest solely through change in the sample-average V_{free} and use this, along with temperature, T, as inputs in eq 3 to compute the film's segmental relaxation time, τ. Part of the approach involves expressing the film's average V_{free} as a simple function of h;

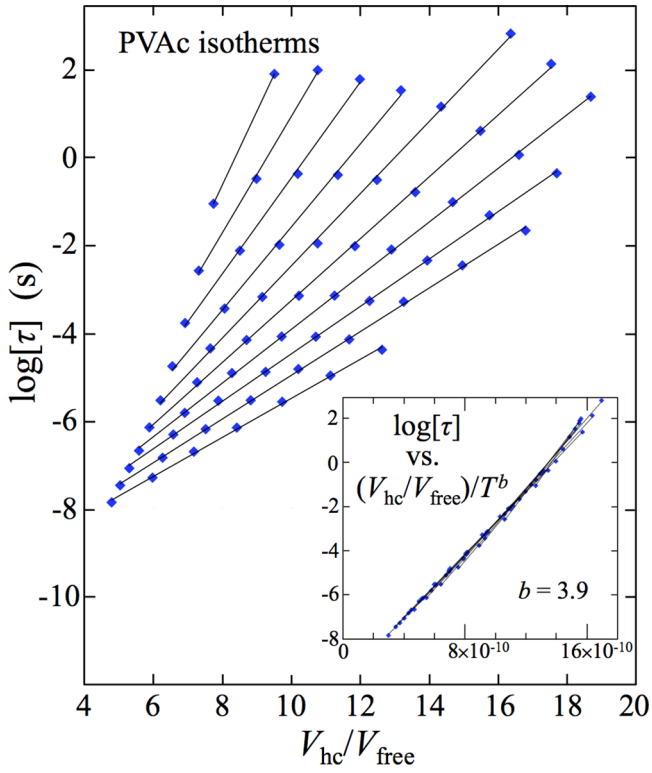

Figure 2. T- and P-dependent α segmental relaxation times for PVAc, plotted as isotherms as a function of inverse relative free volume (V_{hc}/V_{free}); symbols are the experimental data,[60,61] and the lines are the corresponding linear fits. LCL EOS analysis was applied to determine the PVAc V_{hc}/V_{free} values; see section 4 for details. The inset shows that when log τ is plotted as a function of $(V_{hc}/V_{free})/T^b$, with a choice of parameter b = 3.9, the data collapse to a single line (abscissa units K^{-b}). Isotherms range from T = 323 to 413 K in increments of 10 K, and pressure values range from 1 atm up to as high as 400 MPa. Reproduced with permission from ref 19.

upon substitution into eq 3 we therefore obtain an expression, $\tau(T,h)$, for films. We assume that polymer−surface interactions will not change the CFV dynamics parameters (b,T^*,τ_{ref}) from their bulk values; i.e., they are transferable.

We use a simple picture for how an interface affects a film's h-dependent average V_{free}; this is explained here using a free surface as an example, though this picture is equally applicable to other kinds of interfaces. In addition to what follows, the reader is directed to the Appendix for additional (conceptual) details. We propose that in the interior of the sample the local segmental density exhibits a bulklike value but then smoothly decreases to zero at the free surface. Experimental evidence suggests that for a free polymer surface most of the density change occurs just 1 or 2 nm from the interface.[32] Thus, the effective average local segmental density surrounding a segment in, say, the outer 5 nm of the sample is clearly very different from that of the remaining interior, and this contribution results in a net change in the whole-sample average local density and therefore in the sample-averaged dynamics (see note 70 and the Appendix.) We will use a simple weighted average contribution from the two regions (bulk and interfacial) to obtain a result for the overall film's average V_{free} as a function of the film thickness, h. To ultimately arrive at $\tau(T,h)$, we will also express the change in the average film V_{free} with temperature but restrict to the

DOI: 10.1021/acs.macromol.8b01392
Macromolecules 2018, 51, 7924−7941

common experimental scenario where films are at ambient pressure.

Here we note, as an aside, that since the CFV rate model is based on an activation free energy that changes with density (i.e., $\Delta A_{act} \propto n^* \propto 1/V_{free}$), it follows that the confinement effect of a free surface can be identified with a change in activation energy, since thinner films will have a higher average free volume and therefore a lower average activation energy, as they require less cooperativity.

To express the film averaged relative free volume, denoted $(V_{free}/V_{hc})_{film}$, we imagine a film with N segments in total, where N_{int} segments are in the "interface region". The number of segments comprising the interface region (N_{int}) will be fixed regardless of the thickness of the film, and it is N that will vary depending on film thickness. Note this picture is only reasonable as long as films do not become so extremely thin that N is effectively less than N_{int}. We will use $(V_{free}/V_{hc})_{int}$ to denote the average V_{free}/V_{hc} value inside the interface region; for any given T, this intensive property will not change with overall film thickness. Similarly $(V_{free}/V_{hc})_{bulk}$ denotes the local value outside the interface region, and this also will not change with film thickness for any fixed T. The segment-weighted average describing $(V_{free}/V_{hc})_{film}$ is thus given by the following:

$$(V_{free}/V_{hc})_{film} = \left(\frac{N - N_{int}}{N}\right)(V_{free}/V_{hc})_{bulk} + \left(\frac{N_{int}}{N}\right)(V_{free}/V_{hc})_{int}$$
$$= (V_{free}/V_{hc})_{bulk} + \left(\frac{N_{int}}{N}\right)[(V_{free}/V_{hc})_{int} - (V_{free}/V_{hc})_{bulk}] \quad (8)$$

The relative free volume for the bulk polymer at atmospheric pressure, $(V_{free}/V_{hc})_{bulk}$, depends on temperature, and we will want to handle a range of temperature values, so we write its temperature dependence explicitly as

$$(V_{free}/V_{hc})_{bulk} = (V_{free}/V_{hc})_{bulk}^{\circ} + (T - T^{\circ})(\alpha V/V_{hc})_{bulk}^{\circ} \quad (9)$$

where $(V_{free}/V_{hc})_{bulk}^{\circ}$ is the relative free volume at the reference temperature, $T = T^{\circ}$, and $P = 1$ atm. $(\alpha V/V_{hc})_{bulk}^{\circ}$ is the product of the relative volume, V/V_{hc}, and the coefficient of thermal expansion, $\alpha = (1/V)(\partial V/\partial T)_P = (1/V)(\partial V_{free}/\partial T)_P$, at $T = T^{\circ}$ and $P = 1$ atm. The values for $(V_{free}/V_{hc})_{bulk}^{\circ}$ and $(\alpha V/V_{hc})_{bulk}^{\circ}$ are readily calculated, following from the EOS analysis of the bulk polymer melt. Note that $(V_{free}/V_{hc})_{bulk}$ can always be calculated numerically from the EOS at any desired T. However, explicitly writing the (approximate) linear T dependence in eq 9 is more powerful in the analysis.

Substituting eq 9 into (where it appears in the left term of) eq 8 gives

$$(V_{free}/V_{hc})_{film} = (V_{free}/V_{hc})_{bulk}^{\circ} + (T - T^{\circ})(\alpha V/V_{hc})_{bulk}^{\circ} + \left(\frac{N_{int}}{N}\right)[(V_{free}/V_{hc})_{int} - (V_{free}/V_{hc})_{bulk}] \quad (10)$$

Both $(V_{free}/V_{hc})_{bulk}$ and $(V_{free}/V_{hc})_{int}$ are T-dependent. Here we make a simplifying assumption that the T dependence of these two separate quantities will be similar enough that the *difference*, $[(V_{free}/V_{hc})_{int} - (V_{free}/V_{hc})_{bulk}]$, will be constant, independent of temperature. We expect this approximation, which is not essential, but convenient, to be reasonable as long as the change in T is not very large.

We now express N_{int}/N in terms of the overall film thickness, h. The total number of segments in the film, N, is to good approximation, proportional to h. We can write $N = c_\rho h$, where c_ρ is a product of the film area multiplied by the film-average segment density, and this gives $N_{int}/N = N_{int}/(c_\rho h)$. We approximate c_ρ as a constant, which is reasonable because the film's average segment density will not be a strongly varying quantity with h (or even T over limited ranges). For example, it will be shown below that the magnitude of the average segment density will change by about 2% over the span from the thinnest 12 nm film to the large h (bulk) limit. Although this small average segmental density change is the physical reason for the change in dynamics, assuming c_ρ constant, where it appears in this particular mathematical term, is still valid. In the fraction, $N_{int}/N = N_{int}/(c_\rho h)$, $1/h$, and $1/c_\rho$ appear together in a product, so it is the *relative* change in $1/h$ that has far greater impact than any other further impact derived from the (expected, but small) concurrent relative change in $1/c_\rho$.

With N_{int}, c_ρ, and the difference, $[(V_{free}/V_{hc})_{int} - (V_{free}/V_{hc})_{bulk}]$, all assumed constant, we define the single, constant, interface related parameter, $\delta_{free} = [(V_{free}/V_{hc})_{int} - (V_{free}/V_{hc})_{bulk}] \times (N_{int}/c_\rho)$. The film averaged free volume can now be expressed as

$$(V_{free}/V_{hc})_{film} = (V_{free}/V_{hc})_{bulk} + (\delta_{free}/h)$$
$$= (V_{free}/V_{hc})_{bulk}^{\circ} + (T - T^{\circ})(\alpha V/V_{hc})_{bulk}^{\circ} + (\delta_{free}/h) \quad (11)$$

The result is a form such that for any chosen T (i.e., on an isotherm) the difference between the film-averaged free volume and that of the bulk is proportional to $1/h$. This is a key result so it is relevant to point to other work that supports this simple form of behavior. Figure 3 shows some recent atomistic simulation results for freestanding polystyrene films by Zhou and Milner.[71] The specific volumes of the films (all at $T = 420$ K) are plotted as a function of inverse film thickness ($1/h$), and there is a clear linear trend. The difference in specific volume between film and bulk (at the intercept) is of

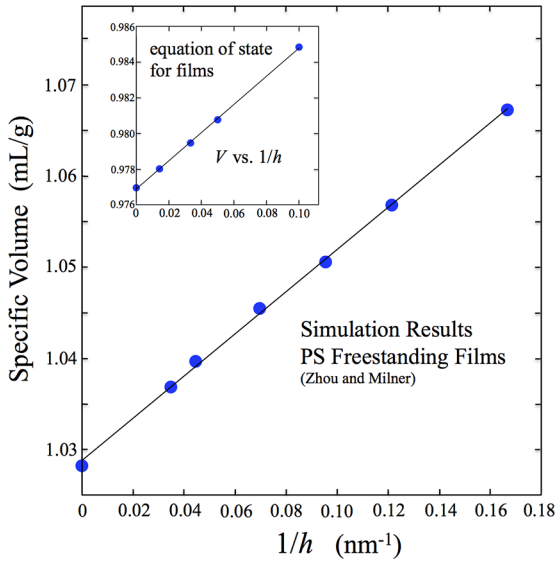

Figure 3. Specific volume of films as a function of inverse film thickness ($1/h$). The main plot shows atomistic simulation results from Zhou and Milner (ref 71) for polystyrene at a temperature of 420 K. The inset shows a similar plot where the specific volumes were calculated from an equation of state designed for films (refs 72 and 73); calculations were for freestanding polystyrene at T just above the bulk T_g.

DOI: 10.1021/acs.macromol.8b01392
Macromolecules 2018, 51, 7924−7941

Table 1. Characterization Parameters for CFV Dynamics Analysis and LCL *PVT* Analysis[a]

		dynamics parameters			LCL *PVT* analysis: parameters and info				
system[b]	T_g (K)	b	T^* (K)	log τ_{ref} (s)	V_{hc} (mL/g)	r/M_w (mol/g)	v (mL/mol)	$-\varepsilon$ (J/mol)	$\langle T_{fit}\rangle$ (K)
present work: CFV fit via just ambient $\tau(T)$ data and *PVT* dT_g/dP data									
P4ClS	391[c]	2.93	634	−12.3	0.7401	0.096 78	7.647	2187	433
PVAc[d]	305	3.67	422	−10.1	0.7583	0.1379	5.499	1805	369
previous work: CFV fit via full $\tau(T,P)$ data sets									
PVAc[d]	305	3.96	420	−10.1	0.7583	0.1379	5.499	1805	369
PVME	242	5.89	272	−8.28	0.8665	0.1306	6.635	1782	341
PMPS	246	2.70	356	−16.4	0.8138	0.1147	7.095	1901	338
PMTS	261	2.22	465	−16.5	0.7177	0.1078	6.658	1717	338
BMPC	241	1.77	536	−17.7	0.8179	0.2242	3.648	1677	328
BMMPC	261	1.61	568	−15.4	0.8338	0.1961	4.252	1858	328
OTP	244	2.71	380	−14.7	0.8202	0.1410	5.817	1720	325
BMP-BOB	231	3.70	266	−10.6	0.7105	0.1655	4.293	1807	326

[a]Parameters: b, T^*, and τ_{ref} are system-dependent parameters for the CFV dynamics expressions. The LCL equation of state molecular parameters are r, the number of segments (occupied lattice sites) per molecule, v, the volume per lattice site, and ε, the segment−segment nonbonded interaction energy. M_w is molecular weight. The hard-core volume, V_{hc}, per molecule, is obtained from the product, rv, and V_{free} is thus defined as $V - V_{hc}$. In the LCL fitting, $\langle T_{fit}\rangle$ is the average temperature of the *PVT* data. [b]System acronyms and information: PVAc: poly(vinyl acetate); PVME: poly(vinyl methyl ether); PMPS: poly(methylphenylsiloxane); PMTS: poly(methyltolylsiloxane); OTP: *o*-terphenyl; BMPS: (1,1′-bis(*p*-methoxyphenyl)cyclohexane; BMMPC: 1,1′-di(4-methoxy-5-methylphenyl)cyclohexane; BMP-BOB: (1-butyl-1-methylpyrrolidinium bis[oxalate]-borate. Details on the temperature and pressure ranges for the modeled dynamics data and *PVT* data for each system can be found in ref 19 and the experimental references listed therein. [c]This T_g value (391 K) corresponds to that of the *PVT* data (see analysis in Figure 5); the T_g value obtained by extrapolation of a VFT fit of the bulk relaxation time data in ref 35 is 398 K, defined by the T where τ = 100 s. [d]There are two PVAc dynamics parameters sets listed in the table. The set corresponding to fitting to the full P-dependent dynamics data set, where b = 3.96, included pressures all the way up to 400 MPa. The fitted b would be closer to 3.67 (the value from the present set) if the range were reduced such that high P's ranged to about 200 MPa or so. The two b values, 3.96 and 3.67, are close, and in general we observe that both values yield a very good data collapse in plots of ln τ vs $V_{hc}/(V_{free}T^b)$ for any choice of range.

course the difference in (specific) *free volume*. The results show that the free volume difference is proportional to $1/h$, in agreement with eq 11. The inset of Figure 3 shows an analogous plot produced using an equation-of-state approach that we had developed earlier to model the volumetric behavior of freestanding films (based on a lattice model in a slab geometry with finite thickness).[72,73] The results correspond to PS films at T just above the bulk T_g. Again, the clear linear trend indicates that the V_{free} difference between film and bulk is proportional to $1/h$.

When the expression for the film-averaged free volume (eq 11) is substituted into the CFV dynamics equation (eq 3), we obtain the model equation (eq 12) below, which yields $\tau(T,h)$ for films at ambient pressure.

$$\ln \tau = \ln \tau_{ref} + \frac{(T^*/T)^b}{(V_{free}/V_{hc})_{bulk}^{\circ} + (T - T^{\circ})(\alpha V/V_{hc})_{bulk}^{\circ} + (\delta_{free}/h)} \quad (12)$$

The parameters, b, T^*, and τ_{ref} are determined from the bulk dynamics characterization, and the additional interface-related parameter, δ_{free}, can be determined from a small amount of dynamics data on the film, even just a single datum point. V_{hc} and the values $(V_{free}/V_{hc})_{bulk}^{\circ}$ and $(\alpha V/V_{hc})_{bulk}^{\circ}$ for the chosen T° are readily calculated from the LCL EOS analysis. Note that eq 12 also makes predictions about the general form of confined system dynamics behavior that is expected to apply to all systems, regardless of the magnitude of δ_{free} value. We will test the form of eq 12 and apply it to P4ClS films in section 5.

4. PREDICTING THE PRESSURE-DEPENDENT DYNAMICS OF P4ClS and PVAc

In this section we will use the CFV model coupled with the locally correlated lattice (LCL) theory equation of state (EOS) to predict the bulk pressure-dependent dynamics of P4ClS. The first step is to analyze pressure−volume−temperature data with the LCL EOS for a compressible one-component system, which is

$$\frac{P}{k_BT} = \left(\frac{1}{v}\right)\ln\left[\frac{V}{V - N_m rv}\right] + \left(\frac{3}{v}\right)\ln\left[\frac{V - (N_m v/3)(r-1)}{V}\right] - \left(\frac{3}{v}\right)\left(\frac{(2r+1)^2}{(V/N_m v) - (1/3)(r-1)}\right) \times \left(\frac{\exp[-\varepsilon/k_BT] - 1}{(1/3)(2r+1)\exp[-\varepsilon/k_BT] + (V/N_m v) - r}\right) \quad (13)$$

N_m is the number of polymer molecules, and k_B is the Boltzmann constant. The molecular parameters are r, the number of segments (occupied lattice sites) per molecule, v, the volume per lattice site, and ε, the segment−segment nonbonded interaction energy. The hard-core (close-packed) volume, V_{hc}, per molecule, is obtained from the product rv. We determine the LCL characterization parameters (r, v, ε) by fitting the EOS to *PVT* data, and from this we can thus calculate $V_{free} = V - V_{hc} = V - N_m rv$. In practice, it is convenient to report V_{hc} per gram, and the free volume values as either relative free volume, V_{free}/V_{hc}, or fractional free volume, V_{free}/V. Note when we evaluate V_{free} at any chosen T,

DOI: 10.1021/acs.macromol.8b01392
Macromolecules 2018, 51, 7924−7941

P point, we use the V value from the LCL EOS, i.e., solving eq 13 at that T, P. Using the actual experimental V value (if available) would give essentially the same V_{free} value whenever the chosen T, P point is inside the PVT data fitting range (because the theoretical and experimental V's are very close). When extending outside the fitting range, however, is where we have found it better to stay consistently within the theory, i.e., using the theoretical V together with the theoretical $V_{hc} = N_m rv$, as any errors will compensate/cancel.

We have fit the LCL EOS to the P4ClS PVT data from Zoller and Walsh[74] (and also to data for PVAc in our previous work[19]). The resulting molecular parameters that will allow us to calculate V_{free} values are tabulated in Table 1. The fit of the EOS to P4ClS is centered on PVT data with an average temperature of 433 K, which is the temperature of the isotherm considered in the film relaxation data from Panagopoulou and Napolitano.[35] In Figure 4, the LCL model curves and corresponding PVT data are shown in the form of $V(T)$ isobars.

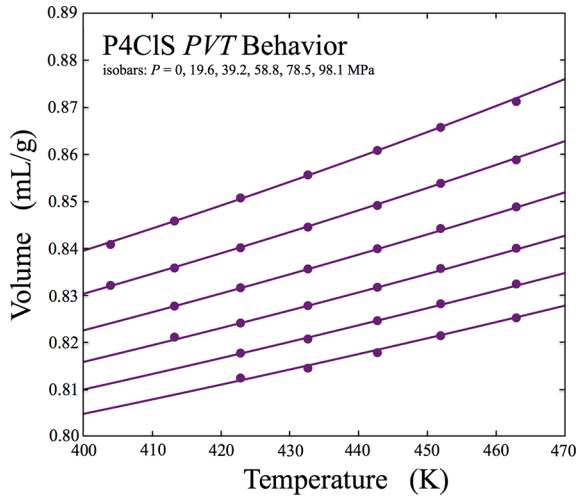

Figure 4. LCL equation-of-state fit to P4ClS PVT data shown in the form of $V(T)$ isobars for P = 0, 19.6, 39.2, 58.8, 78.5, and 98.1 MPa; smooth curves correspond to the LCL model, and the points are the experimental data from Zoller and Walsh.[74] See Table 1 for resulting LCL fitted parameters.

Now that we can calculate V_{free} for any desired T, P point, we consider the bulk dynamics of P4ClS. There is no experimental data available on the pressure-dependent dynamics for P4ClS, so we will apply the CFV model to predict this behavior. This means that we need to parametrize eq 3 ($\ln \tau = \ln \tau_{ref} + (V_{hc}/V_{free})(T^*/T)^b$) for P4ClS using only relaxation data at ambient pressure.

Fitting only ambient pressure $\tau(T)$ dynamics data is not enough to uncouple the complete set of parameters (b, T^*, τ_{ref}) in eq 3. However, having just one additional datum point reflecting information at a different pressure can suffice to accomplish this goal. Here, we will combine ambient pressure $\tau(T)$ data for P4ClS with information about dT_g/dP, as determined from the PVT surface. We will test how well this route works by applying the same analysis to PVAc and then check our predictions for that system against experimental results at different pressures.

To determine dT_g/dP at a given pressure, we will follow a treatment similar to that applied by Roland and Casalini to PVT data for polystyrene,[75] where they fit T_g estimates for each $V(T)$ isobar to a smooth form for $T_g(P)$, the Andersson–Andersson equation,[76] given by

$$T_g = k_1\left(1 + \frac{k_2}{k_3}P\right)^{1/k_2} \tag{14}$$

k_1, k_2, and k_3 are parameters. Our results for P4ClS are shown in Figure 5. The upper panel of the figure shows the estimated

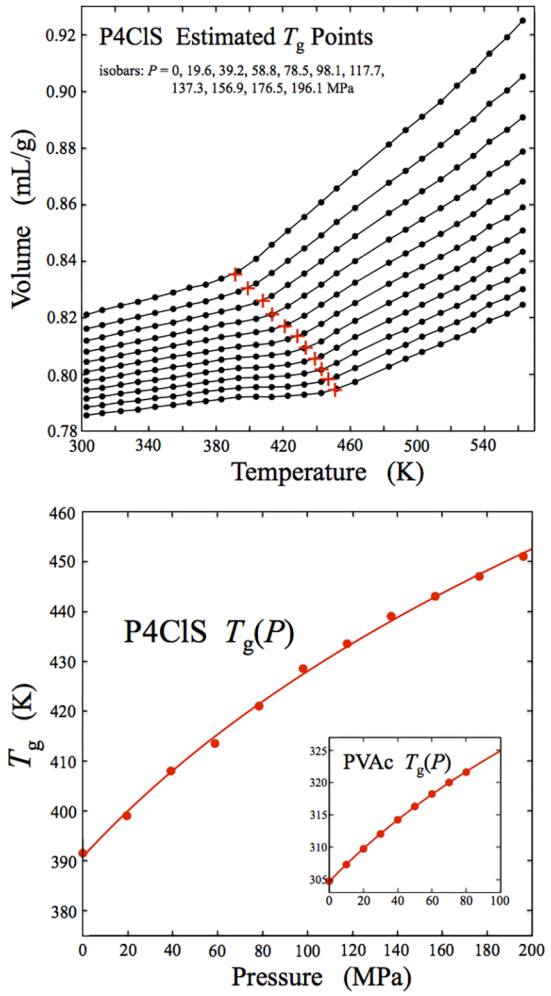

Figure 5. P4ClS PVT data (black points) from Zoller and Walsh[74] where the red "plus signs" indicate the estimated T_g location on each $V(T)$ isobar (upper panel). The resulting fit of T_g vs P to eq 14 is shown in the lower panel. The inset of the lower panel shows the corresponding $T_g(P)$ behavior for PVAc from McKinney and Goldstein.[77]

T_g for each isobar. Using those points, the lower panel of the figure shows the fit to eq 14 (k_1 = 390.8 K, k_2 = 6.791, k_3 = 795.3 MPa). This curve fit gives a dT_g/dP at P = 0 of 0.491 K/MPa, which is a very large value compared to other polymers and small molecules. (See, for example, the values in Table 1 of Roland et al.[1])

In addition to application of this model to P4ClS, we also apply this approach to analysis of poly(vinyl acetate) (PVAc) since in that case we are able verify the CFV predictions against the available P-dependent dynamics data. Thus, the inset in the lower panel of Figure 5 shows corresponding dT_g/dP-related behavior for PVAc where the $T_g(P)$ values are from

DOI: 10.1021/acs.macromol.8b01392
Macromolecules 2018, 51, 7924–7941

the *PVT* analysis of McKinney and Goldstein.[77] The curve for PVAc corresponds to k_1 = 304.6 K, k_2 = 10.08, and k_3 = 1098 MPa and gives the dT_g/dP value at P = 0 of 0.277 K/MPa. The average value for dT_g/dP over the curve is about 0.210 K/MPa, and this is indeed close to the value of 0.220 K/MPa that we connected with in ref 19; this latter value, taken from O'Reilly,[78] was reported as an average over a range of pressure (i.e., not at P = 0).

With the system's dT_g/dP information now at hand, we utilize it as follows: For any two state points having the same relaxation time, τ, the CFV dynamics equation (eq 3) can be used to give

$$(T_2/T_1)^b = (V_{free}/V_{hc})_1/(V_{free}/V_{hc})_2 \quad (15)$$

This "isochronic" expression involves only the model parameter, b, and the T and V_{free}/V_{hc} values at the two points. Next, we make the standard assumption that the T_g point at two different pressures corresponds to the same relaxation time, e.g., 100 s. The particular choice of relaxation time chosen is not important, since it is not required in the equation. The significance of eq 15 is that it allows us to obtain a dynamics parameter (b) from thermodynamic *PVT* data alone. The dynamics parameter γ, applied in thermodynamic scaling treatments, can also be obtained with EOS and dT_g/dP-related information as described in the Roland et al. review.[1]

As noted, we will start with a model parametrization for PVAc to test how well the subsequent predictions for the P-dependent dynamics agree with the (in this case) available P-dependent data.

To obtain the PVAc b parameter using eq 15, we choose two isochronic points: T_g at P = 1 atm (0.1 MPa) and at P = 50 MPa. These P values are typical in our range of application, but other pairs of points within the range could be used just as well; 50 MPa is roughly in the middle of the PVAc $T_g(P)$ data range of ref 77. Using the smooth fit equation (eq 14), we obtain T_1 = 304.7 K and T_2 = 316.2 K for P_1 = 0.1 MPa and P_2 = 50 MPa, respectively. We then use the LCL EOS to solve for the relative free volumes, obtaining $(V_{free}/V_{hc})_1$ = 0.1159 at T_1, P_1, and $(V_{free}/V_{hc})_2$ = 0.1011 at T_2, P_2. Substituting the T and V_{free}/V_{hc} values for the two points into eq 15, we then solve for the b parameter, obtaining the value b = 3.67.

Next we utilize *only* the experimental ambient pressure data for PVAc segmental relaxation times[60,61] and obtain (T^*, τ_{ref}) by fitting eq 3 while keeping the b parameter fixed at 3.67. First, the V_{free} value for each of the T, P (=1 atm) dynamics data points is predicted using the LCL EOS. These results are used to calculate $V_{hc}/(V_{free}T^b)$ for the matching τ values and yield a set of points for the plot of ln τ vs $V_{hc}/(V_{free}T^b)$ values. The linear fit to these points leads to values for T^{*b} and ln τ_{ref} from the best-fit slope and intercept, respectively. The complete set of CFV parameters for bulk PVAc are thus b = 3.67, T^* = 421.6 K, and log τ_{ref} = −10.10. (In the plots, and in tabulating log τ_{ref}, we show the base 10 logarithm of relaxation times to be consistent with common experimental representations, though we note that the values quoted/tabulated for T^* still correspond to using the natural logarithm of eq 3.)

Using this set of parameters gives the model fit to the ambient pressure PVAc segmental relaxation times, plotted in Figure 6 as log τ vs $1/T$ (black model curve with black data points). This PVAc calculation allows us to test the higher P predictions produced by the ambient data fit with the experimental relaxation data collected at higher pressures.[60,61] The blue curves in Figure 6 are the *predicted* relaxation times

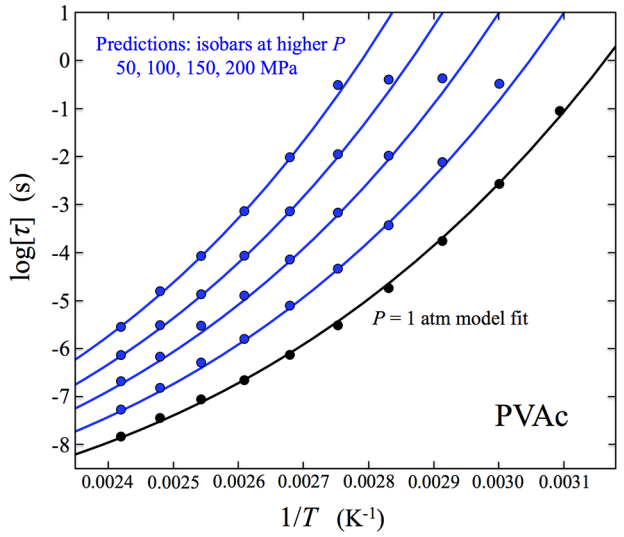

Figure 6. CFV model (eq 3) results for PVAc pressure-dependent dynamics: segmental relaxation times (log τ) as a function of $1/T$ on isobars. The model fit to the ambient pressure (P = 1 atm) isobar is shown by the black curve, and the corresponding data are the black points. The resulting model predictions for higher pressure (isobars of P = 50, 100, 150, and 200 MPa) are shown by the blue curves, and for comparison, the actual experimental data are the blue points. The experimental data are from refs 60 and 61 and the CFV parameters for PVAc are in Table 1.

for isobars at P = 50, 100, 150, and 200 MPa, and the data are the blue points. The agreement between the eq 3 predictions and the actual data is excellent.

Parameterization for P4ClS follows the route described above. For the two isochronic points in eq 15, we use P_1 = 0.1 MPa, T_1 = 390.8 K, and thus $(V_{free}/V_{hc})_1$ = 0.1286 from the LCL analysis of P4ClS and P_2 = 100 MPa, T_2 = 428.0 K, and $(V_{free}/V_{hc})_2$ = 0.0986. (P_1, T_1, and P_2,T_2 came from the eq 14 $T_g(P)$ fit curve; the choice P_2 = 100 MPa is in the middle of the fitted 0-200 MPa $T_g(P)$ data range.) Solving eq 15 leads to a P4ClS b parameter of 2.93. Then, fitting eq 3 to just the ambient pressure segmental relaxation time data (taken from the DS measurements in Panagopoulou and Napolitano[35]), with the fixed b = 2.93, leads to T^* = 633.5 K and log τ_{ref} = −12.32. In the absence of *PVT* data to provide information about the dT_g/dP full model parametrization would require data on P-dependent dynamics.

A plot of the results from the P4ClS ambient data fit, in the form of log τ vs $1/T$, is shown in Figure 7; the curve is the CFV model (eq 3), and the points are the experimental data. The fit is reasonably good; while the three-parameter VFT fit might show somewhat closer agreement with the ambient data, it would not successfully capture the rest of the general pressure-dependent T, V thermodynamic space.

We are now in a position to apply eq 3 to predict the full pressure-dependent dynamics for the bulk P4ClS melt. We reiterate that this process begins with choosing a "grid" of T and P values and predicting the corresponding V_{free} values via the LCL EOS. These T,V_{free} values serve as input into the CFV model equation (eq 3) to get the corresponding predicted τ values for each T, P grid point. The upper panel of Figure 8 shows predictions for segmental relaxation times on P4ClS isobars, plotted as log τ vs $1/T$. The figure shows the isobar at P = 0.1 MPa (black curve), along with the fitted ambient data

DOI: 10.1021/acs.macromol.8b01392
Macromolecules 2018, 51, 7924−7941

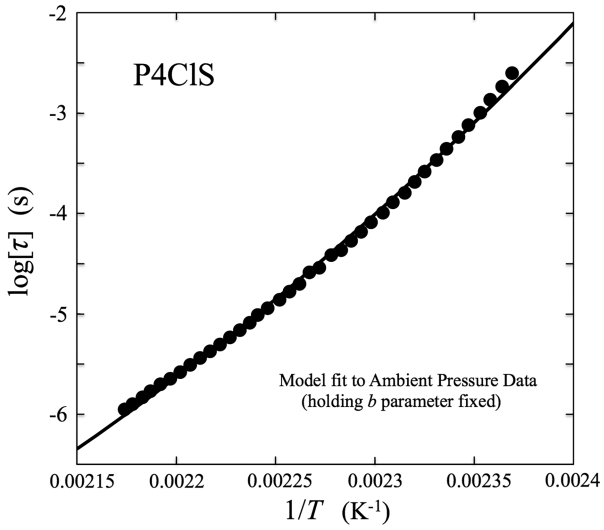

Figure 7. Fit of the CFV model (eq 3) to bulk P4ClS ambient pressure data: segmental relaxation times (log τ) as a function of $1/T$. The model is shown by the curve, and the experimental data[35] are the points. The resulting CFV parameters are in Table 1.

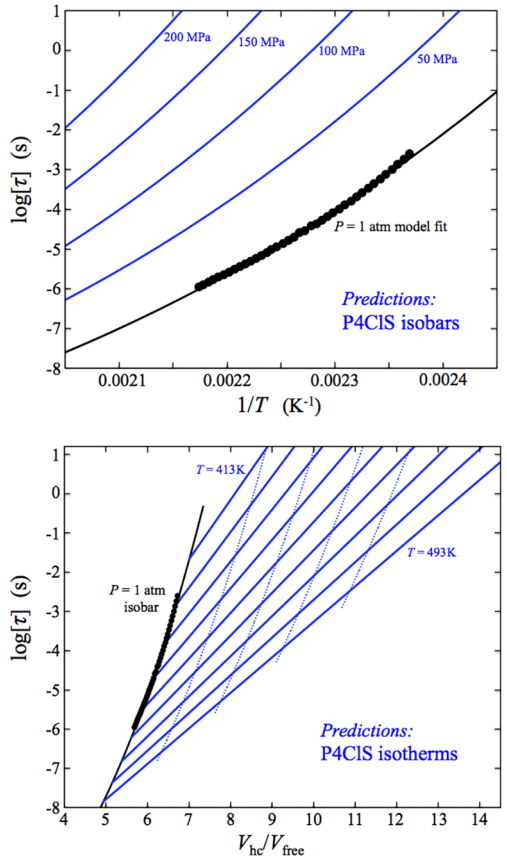

Figure 8. Bulk P4ClS pressure-dependent dynamics; isobars and isotherms. The upper panel shows log τ vs $1/T$ isobars; the black curve is the P = 1 atm isobar, and the black points are the available ambient experimental data[35] to which the CFV model was fit. The blue curves are the model predictions for the P = 50, 100, 150, and 200 MPa isobars. The lower panel shows the model predictions for log τ vs V_{hc}/V_{free} isotherms (solid blue lines) for T = 413 K (top) to 493 K (bottom) in increments of 10 K. Also shown are the P = 1 atm isobar (black model curve and data points) and the P = 50, 100, 150, and 200 MPa isobars (light dotted blue crossing curves).

(points), and the predicted P = 50, 100, 150, and 200 MPa isobars (blue curves).

Comparison between Figures 6 and 8 shows that the increases in log τ with pressure (i.e., the jumps from curve to curve) are larger for P4ClS compared to PVAc. For example, picking any point that starts at about the same relaxation time for both systems, and then going up in pressure to the next isobar at higher P, the increase in log τ for P4ClS is about twice that for PVAc. This is a reflection of the high volume sensitivity for P4ClS, which means it will be relatively sensitive to confinement effects (discussed more fully below).

In the lower panel of Figure 8 we show the model P4ClS predictions in the form of log τ vs V_{hc}/V_{free} isotherms (blue lines). The P = 0.1 MPa isobar (black curve) is included, along with the data (points), as are light dotted blue crossing curves which indicate the locations of the 50, 100, 150, and 200 MPa isobars. As discussed above, the CFV model predicts that on isotherms log τ varies linearly as a function of inverse free volume (V_{hc}/V_{free}), with slopes that increase with decreasing T. All of the systems (experimental and simulated) that we have tested to date (e.g., PVAc in Figure 2) have confirmed this linear behavior, demonstrating that inverse free volume is a natural variable for describing the volume contribution to dynamics. Comparing the P4ClS results in Figure 8 with those for PVAc in Figure 2, we see that the P4ClS isotherms change less dramatically in slope as T decreases; in terms of eq 3, this is a reflection of its lower characteristic b value (2.9, compared to 3.8 for PVAc).

We will return to discuss the predicted P4ClS isotherms when we model the P4ClS film behavior in section 5.1.

The CFV dynamics parameters and LCL EOS parameters from this P4ClS and PVAc analysis are compiled in Table 1, along with parameter values for other systems that we have characterized,[19] for comparison. Consider, first, the b parameter ($b = -(\partial \ln V_{free}/\partial \ln T)_\tau$), which serves to control the relative importance of changing free volume, to that of changing temperature, in that a low b implies more sensitivity to the relative change in V_{free} compared to that of T. For the case of P4ClS, the value of b = 2.93 is on the low side of the spectrum for polymers. This b value is close to those for PMPS and PMTS (also in Table 1).

In density scaling approaches[1,3] (where P-dependent data are collapsed as $\tau = F(TV^\gamma)$, with F being some unknown function of the single combined variable, TV^γ) a similar balancing role is played by $\gamma = -(\partial \ln T/\partial \ln V)_\tau$. A high γ value implies that the system is volume sensitive. In the comprehensive Table 2 of the Roland et al. review,[1] it is relevant then to note how the γ values for PMPS and PMTS are higher than those for all of the other polymers. We find that P4ClS appears to have a similarly strong (relative) sensitivity, although here we assess that in terms of free volume.

Another useful metric for volume sensitivity is the ratio of "effective activation energies" at constant volume and at constant pressure: $E_V/E_P = (\partial \ln \tau / \partial T^{-1})_V/(\partial \ln \tau / \partial T^{-1})_P = 1 - (\partial P/\partial T)_V(\partial T/\partial P)_\tau$.[79] Mathematically, E_V/E_P can vary from 0 to 1, where values close to 1 indicate little sensitivity to changes in volume and values closer to 0 indicate strong sensitivity to changes in volume. Small molecule glass-formers range roughly from a little below 0.4 to about 0.6, while the range for polymers is about 0.55 to 0.85. E_V/E_P values are usually compared for conditions $T = T_g$ (i.e., the experimental glass transition temperature for the system in question) and P = 1 atm. From above, the P4ClS value for $dT_g/dP = (\partial T/\partial P)_\tau$

DOI: 10.1021/acs.macromol.8b01392
Macromolecules 2018, 51, 7924−7941

at T_g is 0.491 K/MPa, and an LCL EOS estimate for $(\partial P/\partial T)_V$ near T_g is 0.85 MPa/K; using these values gives an estimated $E_V/E_P = 0.58$ at T_g. This is quite low for a polymer (not for a small molecule); it is lower than all but three polymers in the Roland et al. table.[1] Over the T range shown in Figure 8 (at P = 1 atm), the CFV model E_V/E_P values (calculated from $(\partial \ln \tau/\partial T^{-1})_V$ and $(\partial \ln \tau/\partial T^{-1})_P$ of the model curves) are similarly low, ranging from 0.59 to 0.61. While the E_V/E_P value of P4ClS is notable for a polymer, its large dT_g/dP value is far more unusual. A system's dT_g/dP value is another metric of volume sensitivity and thus confinement sensitivity (see below).

From the analyses above we conclude that P4ClS is a very free volume sensitive polymer. This has strong implications for its behavior in the film environment, because the essence of the model approach for films eq 12 is based on accounting for the change in average (free) volume on going from bulk to film. A strong response to a change in V_{free} will drive the difference between the bulk and confined dynamics. This connection is not limited to film morphologies, for example Adrjanowicz et al.[22,23] and Tarnacka et al.[24] have experimental results for small molecules confined to nanopores showing that the density of the confined systems was lower than bulk at the same T, and that the changes in the dynamics can be modeled via density scaling.[23] Relevant to our conclusions regarding P4ClS, their work also revealed that the systems with the lowest E_V/E_P values showed the strongest change in relaxation times relative to bulk.

5. RESULTS FOR P4ClS FILMS

5.1. Connecting Pressure and Confinement Effects. In this section we apply the CFV model to data on Al-capped P4ClS films studied via dielectric spectroscopy by Panagopoulou and Napolitano.[35] In particular, we focus on their results for films where the polymer has not strongly adsorbed to the surface (t_{ANN} = 0, before annealing), a situation where the role of the interface is similar to that of a free surface, increasing the local free volume.

In applying the CFV model $\tau(T,h)$ expression (eq 12) to films, we assume that confined dynamics differ from the bulk *only* because the average free volume of the sample has changed. For greater detail regarding our physical picture, see the Appendix. To demonstrate this idea, we show how to interpret ambient pressure film data by using the experimental ln τ values along with the bulk CFV equation, ln $\tau = (V_{hc}/V_{free})(T^*/T)^b + \ln \tau_{ref}$ (eq 3), to predict (i.e., "back-calculate") V_{free} for the film at the experimental temperature. Here we input the experimental τ and T (fixed at 433 K for the data set used here) for the film as measured at different film thicknesses and then solve eq 3 for the film's set of apparent corresponding V_{free} values.[80] The result, pictured as a series red points in Figure 9, is equivalent to extrapolating a bulk isotherm into high enough free volume values that it extends beyond the point where it crosses the atmospheric pressure isobar.

Overall, Figure 9 maps out T, V_{free} space for film and bulk in the form of P4ClS linear log τ vs V_{hc}/V_{free} isotherms (analogous to Figure 8). The points in the figure cover film thicknesses along the T = 433 K isotherm from h = 12 nm up to 212 nm (the latter giving the bulk value as expected). Each isotherm comprises two regions, separated by the P = 1 atm isobar (black dashed curve): the "bulk regime" (solid lines) and the "film regime" (dashed lines). We now use the results along the T = 433 K isotherm to elaborate on this connection

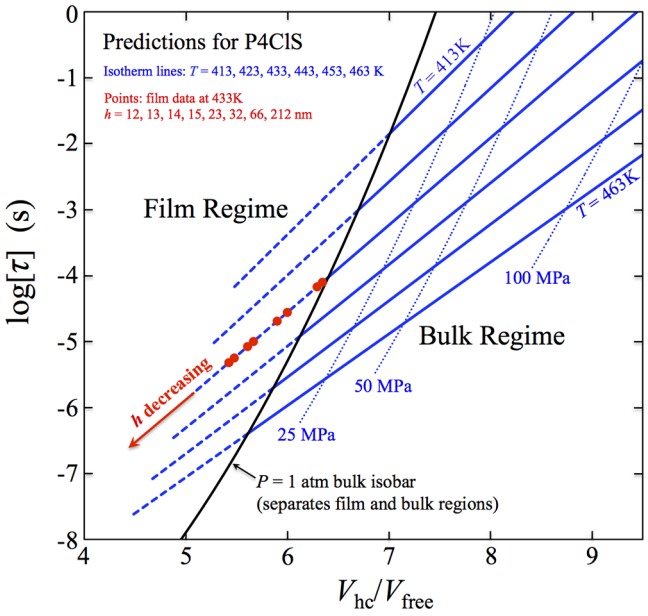

Figure 9. Mapping the film regime and the bulk regime: a generalized P-dependent dynamics picture of segmental relaxation times. The blue lines are CFV model predictions of log τ vs V_{hc}/V_{free} isotherms; T = 413 K (top) to 463 K (bottom) in increments of 10 K. The solid portions of the lines correspond to $P \geq 1$ atm. The extrapolations are shown as dashed lines corresponding to higher V_{free} values associated with films. The bulk ambient P = 1 atm isobar ($P \approx 0$) is shown by the black curve and separates the film and bulk regimes; other isobars (light dotted blue curves) are also shown. The red points were placed (via eq 3) using experimental log τ data for Al-capped P4ClS films[35] on the T = 433 K isotherm. Film thicknesses (left to right) are h = 12, 13, 14, 15, 23, 32, 66, and 212 nm.

between the effect of finite film confinement and that of a pressure change applied to a bulk system:

Start with the log τ value for bulk at P = 1 atm, T = 433 K, which is −4.0. The log τ for an ∼15 nm film at the same temperature and pressure has a value of about −5.1 (e.g., the third and fourth red points from the left along the isotherm at about $V_{hc}/V_{free} \approx 5.6$). The reduction in log τ going from a bulk sample to a 15 nm film is therefore 1.1. Now, we can think of a correspondingly matched *increase* in relaxation time, traveling upward along the same isotherm. This would lead us to the point {log τ = −2.9 and V_{hc}/V_{free} = 7.2} (still at T = 433 K), which appears to sit roughly on the P = 25 MPa isobar. In other words, compared to the change from bulk to a 15 nm film, an equal *magnitude* shift in log τ can be accomplished (with T fixed) by increasing pressure from 0.1 to 25 MPa. We might therefore interpret the shift in relaxation time in going from bulk to 15 nm film as being equivalent to exposing the bulk sample to a "negative" pressure of −25 MPa.

In connecting dynamics under confinement with pressure-dependent dynamics, we thus interpret the "thin film" effect, with its enhanced dynamics, as equivalent to the bulk experiencing a drop in pressure. This key point has been advanced in recent nanopore studies. In Adrjanowicz et al.[22,23] and Tarnacka et al.[24] the change in the dynamics of small molecules confined in nanopores relative to bulk was ascribed to a negative pressure effect. The authors describe a process involving vitrification of interfacial molecules, which leads to negative pressure developing in the pores as T is further decreased. The core molecules in the pores are thus held in

DOI: 10.1021/acs.macromol.8b01392
Macromolecules 2018, 51, 7924−7941

isochoric (constant volume) conditions; since they are at a density less than the corresponding bulk, they exhibit faster dynamics. The results in Kipnusu et al.[81] from dielectric spectroscopy and positron annihilation lifetime spectroscopy also support this picture. Simon et al. studying OTP in nanopores[82] also presented evidence for isochoric conditions to explain the modeled aging behavior; however, they also concluded that negative pressure, alone, did not explain the reason for the T_g shift.

Regardless of the actual value of pressure in the confined system, we believe the most important overall factor is whether there is a sample-averaged density (V_{free}) change compared to bulk, as τ will follow $\tau(T,V_{free})$. Interfaces cause density gradients, which can result in an average density change without invoking negative pressures. For example, across a plane interface there is a density gradient while the pressure is uniform.[30,83] While the present model analyzes data for $\tau(T,h)$ of films at ambient pressure, it is helpful to think of a *hypothetical change* in pressure, in strength and direction, as a convenient and intuitive way to imagine the strength of the perturbation due to confinement.

We now turn to some quantitative results from our analysis of the experimental data. In Table 2 we list both relative free volume, V_{free}/V_{hc}, which is the quantity most rigorously connected to the CFV model (due to direct proportionality with V_{free}), and also fractional free volume, V_{free}/V, which is also a helpful metric when one wants to simply picture what fraction of the space in a sample (of total volume, V) is the part that is the free space.

Table 2. Free Volume Values at T = 433 K for P4ClS Films of Varied Thickness[a]

h (nm)	V_{hc}/V_{free}	V_{free}/V_{hc}	V_{free}/V	V_{free}/V − bulk
bulk	6.399	0.1563	0.1352	0
212	6.344	0.1576	0.1362	0.0010
65.9	6.292	0.1589	0.1371	0.0020
31.6	5.999	0.1667	0.1429	0.0077
22.9	5.899	0.1695	0.1449	0.0098
15.4	5.608	0.1783	0.1513	0.0162
14.6	5.666	0.1765	0.1500	0.0149
13.2	5.477	0.1826	0.1544	0.0192
11.7	5.423	0.1844	0.1557	0.0205

[a]These film-averaged free volume values are calculated from $(V_{free}/V_{hc}) = (T^*/T)^b/\ln[\tau/\tau_{ref}]$ (eq 3), where T = 433 K and the ln τ values correspond to the experimental segmental relaxation times for Al-capped P4ClS films (t_{ANN} = 0) taken from Figure 2 in ref 35. The b, T^*, and τ_{ref} parameters were determined from the bulk P4ClS characterization as described in the text.

As Table 2 shows, the fractional free volume for P4ClS bulk is 13.52%, while the 12 nm film has a deduced fractional free volume (via eq 3) of 15.57%. The absolute difference in percent free volume between film and bulk is thus about 2%, and this corresponds to a *relative* increase in the free space of about 15% (= 2%/13.5%).

The inferred (back-calculated) model free volume changes above provide a test of how well our model assumptions work. For example, we *assume* that the bulk-system-dependent dynamics parameters still apply for films, and we *expect* that that film-averaged free volume values will end up falling on the linear ln τ vs V_{hc}/V_{free} isotherm appropriate to the bulk. This leads to our conclusion that there is an absolute change of 2% (15% relative increase in the space that is free), which seems to be the right order of magnitude. Indeed, our predictions are also quite similar in magnitude to the changes observed in the freestanding PS film simulations of Zhou and Milner. Their results[71] indicate a change from bulk of roughly 2% for films of about 10 nm thickness, and our earlier results using the film EOS[72,73] are consistent, showing about a 1% change.

5.2. Application of the CFV $\tau(T,h)$ Expression to P4ClS Films. We now move to the direct application of eq 12, the CFV model $\tau(T,h)$ expression for films at ambient pressure. Recall that eq 12 has the three bulk parameters, b, T^*, and τ_{ref}, and one, new, interface-related parameter, δ_{free}. The other quantities in eq 12 (V_{hc}, $(V_{free}/V_{hc})_{bulk}^{\circ}$, $(V/V_{hc})_{bulk}^{\circ}$, and α° for the chosen T°) are related to the system thermodynamics and are calculated from the LCL EOS analysis based on thermodynamic information only.

We begin with a test of eq 12 for the condition that $T = T^{\circ}$, in which case eq 12 becomes

$$\frac{(T^*/T^{\circ})^b}{\ln[\tau/\tau_{ref}]} = (V_{free}/V_{hc})_{bulk}^{\circ} + \delta_{free}/h \qquad (16)$$

If this is true, then a plot of $(T^*/T^{\circ})^b/\ln[\tau/\tau_{ref}]$ vs $1/h$ on any isotherm ($T = T^{\circ}$) *should be linear*. The intercept of the line should be equal to $(V_{free}/V_{hc})_{bulk}^{\circ}$, which can be verified by independently calculating that quantity. The slope would yield the new film-related parameter, δ_{free}. We have performed this test using the experimental[35] P4ClS film ln τ and h values as inputs, and $T = T^{\circ}$ = 433 K. The results are plotted in Figure 10.

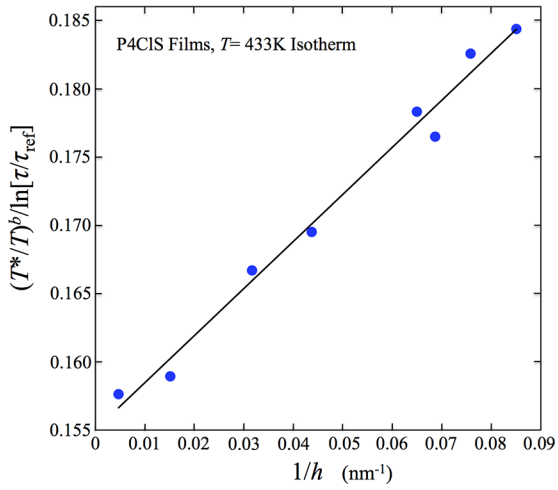

Figure 10. Test of the form of CFV model eq 12 for films: plot of $(T^*/T^{\circ})^b/\ln[\tau/\tau_{ref}]$ vs $1/h$ on the isotherm $T = T^{\circ}$ = 433 K; parameters are in Table 1, and experimental τ data are from ref 35. The $(T^*/T^{\circ})^b/\ln[\tau/\tau_{ref}]$ values on the ordinate yield V_{free}/V_{hc} of a film predicted using the CFV eq 3, for a given τ value and temperature. Equation 12 predicts that this plot should be linear and with an intercept corresponding to the bulk V_{free}/V_{hc} value; both conditions are satisfied.

The plot is indeed linear; the intercept of the best fit line is 0.155, which matches very closely to the correct bulk value from the EOS analysis ($(V_{free}/V_{hc})_{bulk}^{\circ}$ = 0.156). The form of eq 12 for $\tau(T,h)$ results from the combination of two relationships: the fundamental inverse free volume dependence (ln $\tau \sim 1/V_{free}$), which we know is correct for bulk systems, combined with an approximation for the h dependence of free

DOI: 10.1021/acs.macromol.8b01392
Macromolecules 2018, 51, 7924−7941

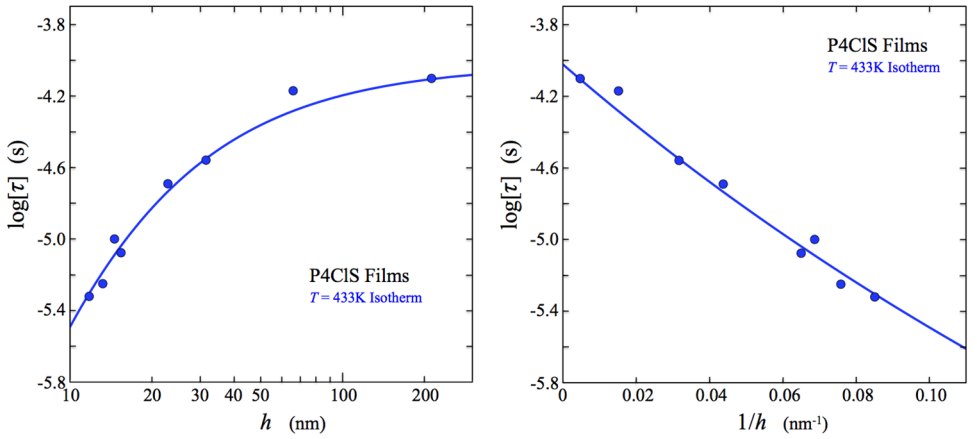

Figure 11. CFV model film results: isothermal relaxation times as a function of film thickness, h (T = 433 K). The left panel shows log τ plotted vs log h, and the right panel shows log τ plotted vs $1/h$. The model curve corresponds to eq 12 using P4ClS bulk parameters and δ_{free} = 0.327 nm, and the points are the experimental Al-capped P4ClS film data from Panagopoulou and Napolitano.[35]

volume in films, $(V_{free}/V_{hc})_{film} = (V_{free}/V_{hc})_{bulk} + \delta_{free}/h$. It appears this simple combination is justified.

Taking δ_{free} from the slope in the Figure 10 plot yields 0.332 nm. If we instead insist on using the known bulk value for the intercept and then refit the points, the result gives δ_{free} = 0.327 nm. This exercise is useful because it leads to the conclusion that a reasonable value for δ_{free} can be obtained using only a single film datum point in conjunction with the known bulk value for the intercept. Note that with enough data on a set of film samples to fit the model, it should be possible to work in "reverse" and determine the bulk parameters (b, T^*, and τ_{ref}).

With the model fully parametrized, we will now analyze the behavior of the eq 12 $\tau(T,h)$ expression in several ways, for example: ln τ as a function of h for any given T (i.e., on an isotherm), ln τ as a function of T for any given h, and T_α as a function of h for any chosen τ value. T_α can be thought of as a dynamic measure of T_g; it is the temperature at which a film of a given h exhibits a particular chosen τ value (i.e., $T_\alpha(h)$ is an isochronic curve).

The left panel of Figure 11 is a plot of the model relaxation time (log τ) as a function of film thickness (h, on a log scale) for P4ClS films on the T = 433 K isotherm at ambient pressure; the right panel correspondingly shows log τ vs inverse film thickness ($1/h$). The curve in each plot corresponds to the model (eq 12), and the points are the data from Panagopoulou and Napolitano.[35] The model form is in very good agreement with the data. As noted above, if we had used just a single one of the film datum points to solve eq 12 for δ_{free}, we would have obtained close to the same model curve, thus predicting the remaining points. That only a single experimental point could suffice provides support for our assertion that the model predicts the correct form of behavior.

We next explore the potential of eq 12 for predicting the effects of changing temperature on film dynamics. Figure 12 shows log τ as a function of h for three isotherms; these include the T = 433 K results along with model *predictions* for the behavior at T = 423 and 443 K. On approaching the large h limit, eq 12 must produce the correct dynamics for the bulk system; therefore, as expected, the predicted curve for the 423 K isotherm (longest bulk relaxation times) lies above that for 433 K, which is above that for 443 K. Note, however, that the steepness of each isotherm is not the same. The model predicts that the effect of decreasing film thickness on relaxation times ($(\partial \ln \tau/\partial h)_T$, for any given h) will be strongest at lower

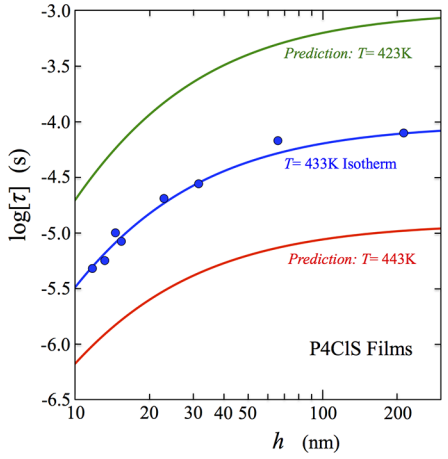

Figure 12. Relaxation times as a function of film thickness, h, predicted using CFV model eq 12 with P4ClS bulk parameters and δ_{free} = 0.327 nm. The middle curve (T = 433 K) shows experimental film data points[35] used in determining the value of the interface parameter, δ_{free}. The other two curves are CFV model predictions for the isothermal film behavior at T = 423 and 443 K; note the sensitivity to change in film thickness is stronger as T decreases.

temperatures. The reason for this follows fundamentally from the CFV eq 3 relationship, in that the magnitude of $(\partial \ln \tau/\partial V_{free})_T$ will become larger as T decreases with V_{free} fixed. For films, V_{free} is a function of film thickness (eq 3 becomes eq 12); therefore, a similar trend holds: at any given h, the tangent to the log τ vs h curve will be larger (have stronger slope) at lower T. This effect can also be seen in the fan-shaped plots of Figures 8 and 9, where the CFV model slopes of the log τ vs V_{hc}/V_{free} linear isotherms increase as T decreases, behavior analogous to that of all previous systems studied.

In Figure 13, we predict the $\tau(T,h)$ behavior plotted in the form of log τ as a function of $1/T$ at ambient pressure for specific chosen film thickness values of h = 60, 30, 20, 15, 12, and 10 nm, along with the ambient pressure bulk curve. These results are predictions because the film data used in the model parametrization came from just a single temperature (433 K), while the plots in Figure 13 predict an entire $\tau(T)$ curve. As expected, the behavior throughout is that the relaxation time increases as T decreases. Note that the model predicts that at any fixed temperature there will be a shorter relaxation time as

DOI: 10.1021/acs.macromol.8b01392
Macromolecules 2018, 51, 7924−7941

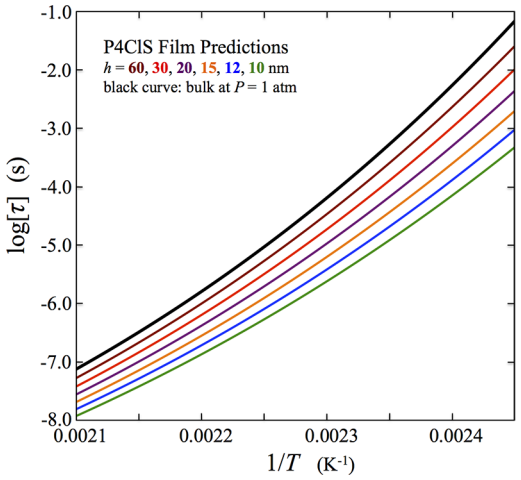

Figure 13. CFV model P4ClS film predictions: log τ vs $1/T$ curves for film thicknesses h = 10, 12, 15, 20, 30, and 60 nm. The ambient pressure curve for P4ClS bulk is shown in black. The model curves correspond to eq 12 using P4ClS bulk parameters and δ_{free} = 0.327 nm.

film thickness decreases. For the system studied here there is an enhancement (positive δ_{free} value) in free volume near the interface. This will increasingly dominate as the film gets thinner, leading to a reduction in τ.

We move now to another important study of the CFV $\tau(T,h)$ behavior. Figure 14 shows model curves for the isochronal temperature, T_α, as a function of film thickness, h, at ambient pressure. Here T_α corresponds to a fixed τ value, chosen to be log $\tau = -4.5$ (τ in seconds). The separate panels show T_α plotted in several different ways, which will be discussed in turn.

The model predicts (panel a) that T_α for P4ClS will decrease by about 17 K on going from bulk to a 10 nm thick film. We emphasize that this prediction, made in the *absence* of any T-dependent film data for the model parametrization, is possible because the CFV model accounts for, and is utilizing, the T, V_{free} behavior of the system's bulk pressure-dependent dynamics. There are no existing experimental data with which to compare the CFV T_α predictions; such data would clearly provide a good means of further testing the model.

Panel b Figure 12 shows that T_α vs $1/h$ appears to be linear, which prompts a closer look at the model eq 12 expression. We cannot directly solve/rearrange eq 12 explicitly for T_α (i.e., for a chosen fixed $\tau = \tau_{fix}$); however, an approximate result can be obtained. First, eq 12 can be solved explicitly for $1/h$, giving

$$\frac{1}{h} = \left(\frac{1}{\delta_{free}}\right)\left(\frac{(T^*/T_\alpha)^b}{\ln[\tau_{fix}/\tau_{ref}]} - (T_\alpha - T^\circ)(\alpha V/V_{hc})_{bulk}^\circ - (V_{free}/V_{hc})_{bulk}^\circ\right) \quad (17)$$

Equation 17 was used in plotting the exact model results for T_α in Figure 12. To approximate a form for T_α, we will utilize derivatives of $1/h$; two routes will be followed.

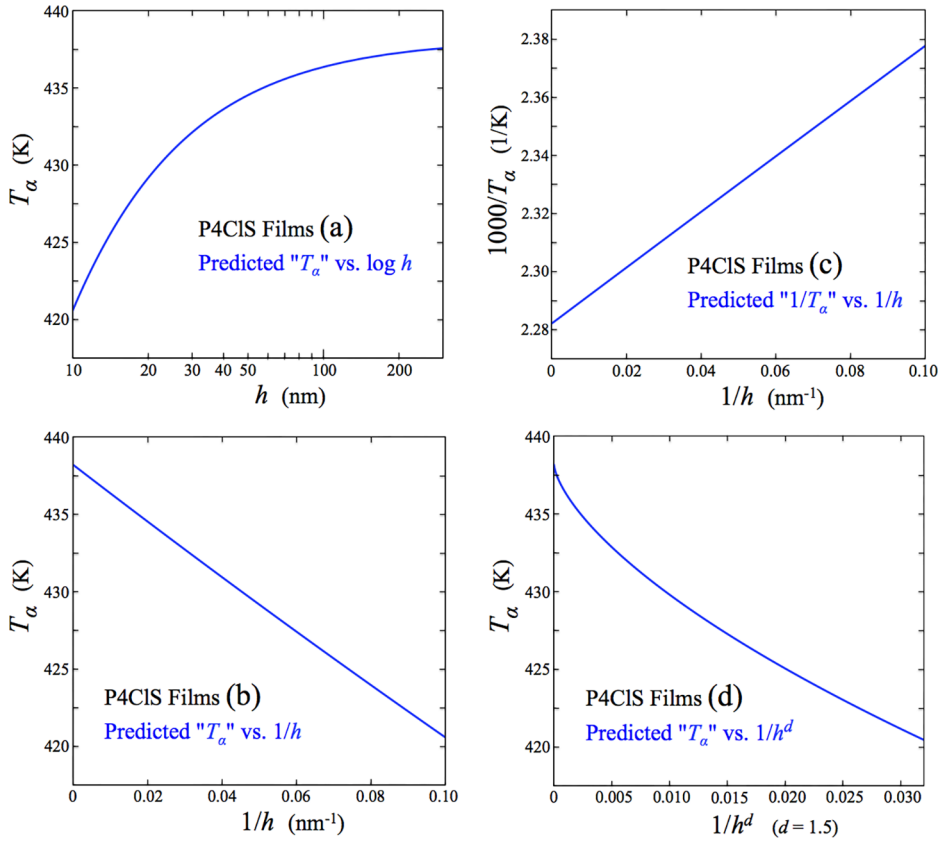

Figure 14. CFV model P4ClS film predictions (using bulk parameters and δ_{free} = 0.327) for the isochronal temperature, T_α (for log $\tau = -4.5$) as a function of film thickness, h. (a) T_α vs log h; (b) T_α vs $1/h$; (c) $1/T_\alpha$ vs $1/h$; (d) T_α vs $1/h^d$ with d = 1.5. T_α suppression on going from bulk to an ~10 nm film is predicted to be in the range of about 17 K.

DOI: 10.1021/acs.macromol.8b01392
Macromolecules 2018, 51, 7924−7941

Panel c in Figure 12, a plot of $1/T_\alpha$ vs $1/h$, is very linear, with the variables $1/h$ and $1/T_\alpha$ both approaching infinity together in the small h limit. Expanding $1/T_\alpha$ about its bulk value and keeping just the term with the first derivative (i.e., using $d(1/T_\alpha)/d(1/h) = 1/[d(1/h)/d(1/T_\alpha)]$, the inverse of the derivative in eq 17) gives the approximate result

$$\frac{1}{T_\alpha} \approx \frac{1}{T_{\alpha,\mathrm{bulk}}} + \left(\frac{(bT^*)(T^*/T_{\alpha,\mathrm{bulk}})^{b-1}}{\ln[\tau_{\mathrm{fix}}/\tau_{\mathrm{ref}}]} + T_{\alpha,\mathrm{bulk}}{}^2 (\alpha V/V_{\mathrm{hc}})_{\mathrm{bulk}}{}^\circ \right)^{-1} \left(\frac{\delta_{\mathrm{free}}}{h} \right) \tag{18}$$

an expression that is linear in $1/h$. The corresponding expansion in T_α using the first derivative, $dT_\alpha/d(1/h)$, leads to an analogous approximate result also linear in $1/h$.

$$T_\alpha \approx T_{\alpha,\mathrm{bulk}} - \left(\frac{(b/T^*)(T^*/T_{\alpha,\mathrm{bulk}})^{b+1}}{\ln[\tau_{\mathrm{fix}}/\tau_{\mathrm{ref}}]} + (\alpha V/V_{\mathrm{hc}})_{\mathrm{bulk}}{}^\circ \right)^{-1} \left(\frac{\delta_{\mathrm{free}}}{h} \right) \tag{19}$$

Equation 18 is a very accurate approximation. Over the entire range in Figure 14, from bulk (T_α = 438 K) to h = 10 nm (T_α = 421 K), the actual (tangent) slope of $1/T_\alpha$ vs $1/h$ changes by less than 2%. So eq 18, which approximates the slope as constant, works well. In the case of T_α vs $1/h$, the actual (tangent) slope changes a bit more, but still by only 9%. So the form of eq 19, which produces a linear slope as well, still represents a reasonable approximate relationship.

The expressions for T_α (both eqs 18 and 19) clearly demonstrate that those systems with higher free volume sensitivity (low b, low E_V/E_P, high γ), will show stronger sensitivity to confinement. With $T^*/T_{\alpha,\mathrm{bulk}} > 1$, lower b values will result in T_α vs $1/h$ slopes with larger magnitude and thus a stronger change in the dynamics (T_α) as $1/h$ increases (h decreases). As noted above, this connection of the confinement effect to the volume sensitivity in a bulk system's pressure-dependent dynamics is the same point that has been emphasized in the recent nanopore results of Adrjanowicz et al.[22] and Tarnacka et al.[24]

The eq 19 form for T_α leads to an interesting comparison regarding the glass transition behavior of polymer films. The isochronal temperature, T_α (e.g., at τ = 100 s, or defined at other τ values), can be viewed as a "dynamic measure" of the glass transition temperature, T_g, because it directly reflects the segmental motion. By contrast, a "thermodynamic measure" of T_g is defined by the point where there is a change in the T dependence of a first-order thermodynamic property, e.g., when it is probed via calorimetry, dilatometry, ellipsometry, etc. For bulk systems, "thermodynamic T_g" and "dynamic T_g" generally agree with each other in marking where a system falls out of equilibrium and forms the glass. However, for the case of confined systems, there is growing evidence that these two measures become decoupled and thus are not necessarily equivalent.[6,84−90] For example, it appears as T decreases below the point of effective segmental mobility (segmental relaxation), confined systems can still be able to maintain thermodynamic equilibrium (ref 90 presents a possible mechanism). Therefore, results generally show that the thermodynamic T_g is more strongly affected by confinement than is the dynamic T_g.

Equation 19 predicts that "dynamic T_g" goes as $T_\alpha = T_{\alpha,\mathrm{bulk}} - [\mathrm{constant}]/h$, and it is natural to contrast this with the empirical form proposed by Keddie et al.,[91] $T_g = T_{g,\mathrm{bulk}} - [\mathrm{constant}]/h^d$. The latter was shown to describe thermodynamically measured T_g values for supported polystyrene films. Correlating a large set of results, Keddie et al.[91] reported a value of d = 1.8, later updated to d = 1.28;[92,93] using another set of results, Ellison et al. reported a value of d = 1.63. The "d" predicted by the CFV model (eq 19) is, of course, unity. While there is some variability in the experimental thermodynamically measured T_g results, a value of $d > 1$ is clear. This appears consistent with the general observations noted above that thermodynamic T_g is more strongly affected by confinement than the dynamic measure of T_g.[86−88] We therefore propose (at least for films that are not "too thin") that d = 1 should be reasonable for dynamic T_g (T_α), while we might expect $d > 1$ to be more common for thermodynamic T_g. (The latter $d > 1$ behavior follows perhaps because a confined system can resort to further mechanisms other than segmental relaxation to maintain equilibrium.) To verify whether the thermodynamic T_g behavior is actually distinguishable from the CFV model T_α trends, over the given bulk to h = 10 nm range, we have plotted the model T_α against the variable, $1/h^d$, using a value of d = 1.5 (panel d of Figure 14); the visually noticeable nonlinearity of the plot illustrates the difference between these two forms of behavior.

Finally, it is useful to note that Hanakata et al.[94] proposed a form for the T_g dependence of films varying linearly with $1/h$ (d = 1), similar to eq 19. Their result was based on an analogy to the Gibbs−Thomson equation for melting T under confinement.[27,95,96] In addition, they demonstrated that this form agreed with their simulation results, and relevant to the argument above, these T_g values were "dynamic T_g's", corresponding to segmental relaxation times extrapolated to large τ via fitting to the VFT equation.

6. SUMMARY AND CONCLUSIONS

The results in this work illuminate a connection between the roles of changing pressure and confinement on dynamic relaxation in thin films. This is accomplished using the cooperative free volume (CFV) model rate equation, which can describe and predict segmental relaxation times for glass-forming melts, $\tau(T,V_{\mathrm{free}})$, as a function of two thermodynamic variables: temperature (T) and free volume (V_{free}). The latter is a rigorously defined quantity, predicted using our locally correlated lattice (LCL) theory's equation of state.

Films at some given temperature, T, and ambient pressure will have an average density (V_{free}) that is different from that of the bulk, and our results point to this difference as the cause of the change in the dynamics. A model such as ours, which captures P-dependent dynamics, can account for *independent* changes in T, V (or equivalently T, V_{free}), which is a key reason for the ability of the CFV model to treat films. Indeed, using the film's V_{free} value, which depends on thickness, our P-dependent CFV model leads to the correct dynamics behavior for the film at the experimental temperature and leads us to predict the behavior at other temperatures.

The steps in extending the CFV $\tau(T,V_{\mathrm{free}})$ equation to films are as follows: (1) We assume that the most important effect of confinement is that the presence of an interface serves to change the average density (V_{free}) compared to bulk. (2) We formulate a simple thickness-dependent expression for the average V_{free} of a film; the result is that at any given T the

DOI: 10.1021/acs.macromol.8b01392
Macromolecules 2018, 51, 7924−7941

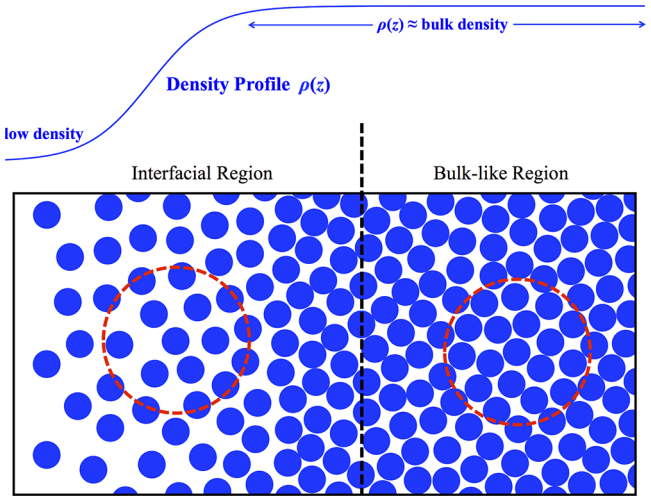

Figure 15. Diagram showing segments (or small molecules) in the two regions of a finite sample/film having a free surface (on the left). The dashed line separates the interfacial and bulklike regions. The corresponding local density profile, $\rho(z)$, is shown at the top. The dashed circle represents/covers the region over which a central segment would be influenced by the presence of its surrounding neighboring segments and leads to the relevant density (free volume) contribution to dynamics to be averaged over each segment. See the Appendix for additional details.

difference in V_{free} between film and the corresponding bulk is proportional to $1/h$, where a single T-independent parameter (δ_{free}) characterizes the strength to which the interface alters V_{free}. (3) We substitute this $V_{free}(h)$ into our CFV $\tau(T,V_{free})$ equation which has been characterized to describe the bulk P-dependent dynamics for the given polymer; we assume that the bulk CFV parameters for the polymer are *transferable* to the film.

Analysis of experimental data (available only at T = 433 K) for Al-capped P4ClS films reveals that the relaxation time results shift with decreasing film thickness in a fashion analogous as to what might be expected if the pressure of the system were decreased. When the experimental log τ points collected for the set of films at different thicknesses are positioned in the CFV log τ versus V_{hc}/V_{free} plot generated for the bulk, the film data fall on the existing isotherm for T = 433 K that has been extrapolated to lie below the P = 1 atm isobar. This makes the connection between film thickness and pressure quite clear; for example, the change in relaxation time at 433 K for a 15 nm film, relative to the bulk result, is similar to what would be expected for a P decrease of about 25 MPa.

We also determine that the percent free volume in the 12 nm film (T = 433 K) is about 15.57% compared to a value of 13.52% for the bulk. The fact that P4ClS bulk dynamics are very sensitive to (free) volume changes (shown here to have low E_V/E_P and low CFV b parameter values) leads directly to there being strong sensitivity of the dynamics to confinement effects, and this can be shown analytically by the form of the CFV model film equation.

The data analysis leads to a set of V_{free} values associated with the different film thicknesses, which allows us to test the CFV prediction for the functional relationship between T, τ, V_{free}, and film thickness, h. In particular, the form for the τ vs h behavior for films at constant T matches the experimental data very well. Indeed, the quality of the model-to-data match shows that only a single film datum can suffice to quantify the one interface parameter (δ_{free}).

We are thus able to predict the behavior at other temperatures, which can be tested in the future. One key prediction is that the sensitivity to confinement ($(\partial \ln \tau/\partial h)_T$) will increase as T is decreased. We also predict that the isochronal T_α (i.e., the temperature required to maintain a constant relaxation time) is a linear function of inverse film thickness ($1/h$). We note that these predictions have been made for the T *dependence of film dynamics*, having characterized the system *using data at a single temperature*.

Our work emphasizes that capturing the effect of confinement on glassy dynamics requires data for and understanding of P-dependent dynamics. Most models require full sets of P-dependent dynamics data for parametrization. The CFV model, which makes use of the thermodynamic free volume, requires fewer dynamics-related parameters and so can be parametrized for an experimental system for which fewer dynamics data are available. Indeed, we demonstrate in this paper that the CFV model holds predictive power when parametrized using *only* ambient dynamics data and PVT data.

APPENDIX. A CONCEPTUAL PICTURE FOR MODELING FREE VOLUME IN NONUNIFORM ENVIRONMENTS

In the approach described in this paper we assume that there is a difference in relative free volume between the interfacial and the bulk regions, characterized by δ_{free}, our single film-relevant parameter. Although we do not aim to predict δ_{free} values, it may be helpful to describe how we interpret the average relative free volume of the inhomogeneous interfacial region in the film. To aid in this, we include a diagram, Figure 15.

We imagine (the model *does not require doing the calculation*) averaging the local segment density, $\rho(z)$, inside a circle based at each segment's location; the result for each segment is then averaged again, this time over all the segments in the entire interfacial region. Say the result of this second average is a density value of "X". Next, consider a homogeneous sample of the same material at a density of "X". Using the LCL characterization of the material, we can predict the relative free volume associated with a homogeneous sample of density "X", and that is the value we think of being associated with the inhomogeneous interface region.

There will be some appropriate *average* distance (average circle radius) to use in this procedure. This average length scale (upon which the value of density "X" will depend) accounts for the neighbor environment around a central point, an effect that is physically relevant for the segmental dynamics at that position, and cannot be reflected by the simple value of $\rho(z)$ alone. The length scale is expected to be system-dependent and to satisfy the condition where the average observed relaxation time in the inhomogeneous interface region is the same as that of the corresponding homogeneous reference environment at density "X" (i.e., the same τ would be calculated via CFV eq 3 using the V_{free} for homogeneous density "X"). Note also how this picture fits well with use in an equation that describes homogeneous bulk dynamics. The definition is thus self-consistent within CFV and the LCL EOS. Technically, the length scale should change (decrease) as one heads away from the interior out to lower density due to decreasing cooperativity. What we describe here is the *average* length scale; one might expect its value to be on the order of 1, 2, 3, or so nm.

DOI: 10.1021/acs.macromol.8b01392
Macromolecules 2018, 51, 7924−7941

The "film-average relative free volume" that we speak of is then the average of the relative free volume of the interface region (defined by its homogeneous equivalent described above) together with the value of the bulklike region, weighted by the number of segments in each region. This picture provides a conceptual way to map to a relative free volume value that is appropriate for describing the volume contribution to dynamics in a nonuniform environment.

We emphasize that application of the CFV model does not require undertaking this average and thus does not involve choosing a length scale for averaging. The practical implication is that the model will simply breakdown when a film is so extremely thin that there is no bulklike region left. Note that the given length scale has pushed the boundary (dashed line in the diagram), from where $\rho(z)$ reached a bulklike value, to some distance further into the interior. It can thus be expected from this picture that the gradient in relaxation should be wider than the density gradient, as observed in simulations.[28] With enough experimental data available to identify the film thickness value where the model breaks down, along with an approximate knowledge of $\rho(z)$, it should be possible to determine the length scale.

Finally, a few more words on the boundary: The boundary cannot be moved so far away from the interior that segments affected by the presence of the gradient get assigned (wrongly) into the bulk region. However, the boundary could be moved arbitrarily in the other direction, provided that the film is thick enough that a bulk region still remains. This change of the boundary position will not affect the value of the δ_{free} parameter and thus the film's overall confinement effect. Here is the reasoning as to why δ_{free} remains a constant even though N_{int} could be changed to define a different size for the interface region:

Consider two different definitions for the interface region, "A" and "B". Imagine that "A" is our original definition where $N_{int} = N_{int,A}$, and then, for "B", we double the size of the interface region. Now, this means that if the "edge" of the "A" interface region was already bulklike (which we have assumed, because outside the region must be all bulklike), then certainly increasing the interface region boundary to the "B" definition only adds a bulklike contribution to the value of $(V_{free}/V_{hc})_{int}$. Therefore, we have

$$(V_{free}/V_{hc})_{int,B} = (1/2)(V_{free}/V_{hc})_{int,A} + (1/2)(V_{free}/V_{hc})_{bulk}$$

and

$$N_{int,B} = 2N_{int,A}$$

Thus

$$\begin{aligned}\delta_{free,B} &= [(V_{free}/V_{hc})_{int,B} - (V_{free}/V_{hc})_{bulk}] \times (N_{int,B}/c_\rho)\\ &= [(1/2)(V_{free}/V_{hc})_{int,A} + (1/2)(V_{free}/V_{hc})_{bulk}\\ &\quad - (V_{free}/V_{hc})_{bulk}] \times (2N_{int,A}/c_\rho)\\ &= (1/2)[(V_{free}/V_{hc})_{int,A} - (V_{free}/V_{hc})_{bulk}] \times (2N_{int,A}/c_\rho)\\ &= [(V_{free}/V_{hc})_{int,A} - (V_{free}/V_{hc})_{bulk}] \times (N_{int,A}/c_\rho)\\ &= \delta_{free,A}\end{aligned}$$

Again, the above argument is meant to amplify the physical picture of the model; no decision on placing the boundary and no averaging process are required. The CFV model expression will just simply no longer apply to the observed/experimental results once films become too thin (i.e., so thin that there no longer remains any bulklike layer). The results in this article indicate the model is applicable at least down to films of 12 nm. Considering that the films have two interfaces, this would imply that a 6 nm wide interfacial region is enough to at least reasonably contain the segments that are affected by the presence of the interface. Note further that this region is indeed significantly wider than the expected 1−2 nm range over which $\rho(z)$ might change for a free surface, as the gradient in relaxation is expected to be wider than the gradient in the local density profile, $\rho(z)$.

AUTHOR INFORMATION

Corresponding Author

*E-mail: jane.lipson@dartmouth.edu (J.E.G.L.).

ORCID

Jane E. G. Lipson: 0000-0002-0177-9373

Notes

The authors declare no competing financial interest.

ACKNOWLEDGMENTS

We gratefully acknowledge the financial support provided by the National Science Foundation (DMR-1708542). JEGL also acknowledges the Radcliffe Institute for Advanced Study at Harvard University. We also acknowledge Simone Napolitano for very helpful discussions.

REFERENCES

(1) Roland, C.; Hensel-Bielowka, S.; Paluch, M.; Casalini, R. Supercooled dynamics of glass-forming liquids and polymers under hydrostatic pressure. *Rep. Prog. Phys.* **2005**, *68*, 1405−1478.

(2) Roland, C. M. Relaxation Phenomena in Vitrifying Polymers and Molecular Liquids. *Macromolecules* **2010**, *43*, 7875−7890.

(3) Floudas, G.; Paluch, M.; Grzybowski, A.; Ngai, K. *Molecular Dynamics of Glass-Forming Systems - Effects of Pressure*; Springer: Berlin, 2011.

(4) Floudas, G. *Broadband Dielectric Spectroscopy*; Springer: Berlin, 2003.

(5) Cangialosi, D. Dynamics and thermodynamics of polymer glasses. *J. Phys.: Condens. Matter* **2014**, *26*, 153101.

(6) Napolitano, S.; Glynos, E.; Tito, N. B. Glass transition of polymers in bulk, confined geometries, and near interfaces. *Rep. Prog. Phys.* **2017**, *80*, 036602.

(7) Stillinger, F. H.; Debenedetti, P. G. Glass Transition Thermodynamics and Kinetics. *Annu. Rev. Condens. Matter Phys.* **2013**, *4*, 263−285.

(8) Debenedetti, P. G.; Stillinger, F. H. Supercooled liquids and the glass transition. *Nature* **2001**, *410*, 259−267.

(9) Ediger, M.; Angell, C.; Nagel, S. Supercooled liquids and glasses. *J. Phys. Chem.* **1996**, *100*, 13200−13212.

(10) Angell, C.; Ngai, K.; McKenna, G.; McMillan, P.; Martin, S. Relaxation in glassforming liquids and amorphous solids. *J. Appl. Phys.* **2000**, *88*, 3113−3157.

(11) Angell, C.; Borick, S. Specific heats C-p, C-v, C-conf and energy landscapes of glassforming liquids. *J. Non-Cryst. Solids* **2002**, *307-310*, 393−406.

(12) Martinez, L. M.; Angell, C. A. A thermodynamic connection to the fragility of glass-forming liquids. *Nature* **2001**, *410*, 663−667.

(13) Ferrer, M.; Lawrence, C.; Demirjian, B.; Kivelson, D.; Alba-Simionesco, C.; Tarjus, G. Supercooled liquids and the glass transition: Temperature as the control variable. *J. Chem. Phys.* **1998**, *109*, 8010−8015.

DOI: 10.1021/acs.macromol.8b01392
Macromolecules 2018, 51, 7924−7941

(14) McKenna, G. B. A brief discussion: Thermodynamic and dynamic fragilities, non-divergent dynamics and the Prigogine-Defay ratio. *J. Non-Cryst. Solids* **2009**, *355*, 663−671.
(15) Mckenna, G. B.; Simon, S. L. Challenges in the Dynamics and Kinetics of Glass-Forming Polymers. *Macromolecules* **2017**, *50*, 6333−6361.
(16) Berthier, L.; Biroli, G. Theoretical perspective on the glass transition and amorphous materials. *Rev. Mod. Phys.* **2011**, *83*, 587−645.
(17) Dyre, J. C. Colloquium: The glass transition and elastic models of glass-forming liquids. *Rev. Mod. Phys.* **2006**, *78*, 953−972.
(18) Chen, K.; Saltzman, E. J.; Schweizer, K. S. Segmental dynamics in polymers: from cold melts to ageing and stressed glasses. *J. Phys.: Condens. Matter* **2009**, *21*, 503101.
(19) White, R. P.; Lipson, J. E. G. How Free Volume Does Influence the Dynamics of Glass Forming Liquids. *ACS Macro Lett.* **2017**, *6*, 529−534.
(20) White, R. P.; Lipson, J. E. G. Explaining the T,V-dependent dynamics of glass forming liquids: The cooperative free volume model tested against new simulation results. *J. Chem. Phys.* **2017**, *147*, 184503.
(21) White, R. P.; Lipson, J. E. G. Pressure-Dependent Dynamics of Polymer Melts from Arrhenius to Non-Arrhenius: The Cooperative Free Volume Rate Equation Tested against Simulation Data. *Macromolecules* **2018**, *51*, 4896−4909.
(22) Adrjanowicz, K.; Kaminski, K.; Koperwas, K.; Paluch, M. Negative Pressure Vitrification of the Isochorically Confined Liquid in Nanopores. *Phys. Rev. Lett.* **2015**, *115*, 265702.
(23) Adrjanowicz, K.; Kaminski, K.; Tarnacka, M.; Szklarz, G.; Paluch, M. Predicting Nanoscale Dynamics of a Glass-Forming Liquid from Its Macroscopic Bulk Behavior and Vice Versa. *J. Phys. Chem. Lett.* **2017**, *8*, 696−702.
(24) Tarnacka, M.; Kipnusu, W. K.; Kaminska, E.; Pawlus, S.; Kaminski, K.; Paluch, M. The peculiar behavior of the molecular dynamics of a glass-forming liquid confined in native porous materials - the role of negative pressure. *Phys. Chem. Chem. Phys.* **2016**, *18*, 23709−23714.
(25) Ediger, M. D.; Forrest, J. A. Dynamics near Free Surfaces and the Glass Transition in Thin Polymer Films: A View to the Future. *Macromolecules* **2014**, *47*, 471−478.
(26) Richert, R. Dynamics of Nanoconfined Supercooled Liquids. *Annu. Rev. Phys. Chem.* **2011**, *62*, 65−84.
(27) Alcoutlabi, M.; McKenna, G. Effects of confinement on material behaviour at the nanometre size scale. *J. Phys.: Condens. Matter* **2005**, *17*, R461−R524.
(28) Simmons, D. S. An Emerging Unified View of Dynamic Interphases in Polymers. *Macromol. Chem. Phys.* **2016**, *217*, 137−148.
(29) Baschnagel, J.; Varnik, F. Computer simulations of supercooled polymer melts in the bulk and in-confined geometry. *J. Phys.: Condens. Matter* **2005**, *17*, R851−R953.
(30) Sanchez, I. C. *Physics of Polymer Surfaces and Interfaces*; Butterworth: Greenwich, CT, 1992.
(31) Poser, C. I.; Sanchez, I. C. Surface-Tension Theory of Pure Liquids and Polymer Melts. *J. Colloid Interface Sci.* **1979**, *69*, 539−548.
(32) Dee, G.; Sauer, B. The surface tension of polymer liquids. *Adv. Phys.* **1998**, *47*, 161−205.
(33) Napolitano, S.; Rotella, C.; Wubbenhorst, M. Can Thickness and Interfacial Interactions Univocally Determine the Behavior of Polymers Confined at the Nanoscale? *ACS Macro Lett.* **2012**, *1*, 1189−1193.
(34) Napolitano, S.; Capponi, S.; Vanroy, B. Glassy dynamics of soft matter under 1D confinement: How irreversible adsorption affects molecular packing, mobility gradients and orientational polarization in thin films. *Eur. Phys. J. E: Soft Matter Biol. Phys.* **2013**, *36*, 61.
(35) Panagopoulou, A.; Napolitano, S. Irreversible Adsorption Governs the Equilibration of Thin Polymer Films. *Phys. Rev. Lett.* **2017**, *119*, 097801.
(36) Tarnacka, M.; Kaminski, K.; Mapesa, E. U.; Kaminska, E.; Paluch, M. Studies on the Temperature and Time Induced Variation in the Segmental and Chain Dynamics in Poly(propylene glycol) Confined at the Nanoscale. *Macromolecules* **2016**, *49*, 6678−6686.
(37) Doolittle, A. K. Studies in Newtonian Flow 0.2. the Dependence of the Viscosity of Liquids on Free-Space. *J. Appl. Phys.* **1951**, *22*, 1471−1475.
(38) Vogel, H. The temperature dependence law of the viscosity of fluids. *Phys. Z.* **1921**, *22*, 645−646.
(39) Fulcher, G. S. Analysis of recent measurements of the viscosity of glasses. *J. Am. Ceram. Soc.* **1925**, *8*, 339−355.
(40) Tammann, G.; Hesse, W. The dependancy of viscosity on temperature in hypothermic liquids. *Z. Anorg. Allg. Chem.* **1926**, *156*, 245.
(41) Cohen, M. H.; Turnbull, D. Molecular Transport in Liquids and Glasses. *J. Chem. Phys.* **1959**, *31*, 1164−1169.
(42) Williams, M. L.; Landel, R. F.; Ferry, J. D. Mechanical Properties of Substances of High Molecular Weight 0.19. the Temperature Dependence of Relaxation Mechanisms in Amorphous Polymers and Other Glass-Forming Liquids. *J. Am. Chem. Soc.* **1955**, *77*, 3701−3707.
(43) Ferry, J. D. *Viscoelastic Properties of Polymers*; Wiley: New York, 1970.
(44) White, R. P.; Lipson, J. E. G. Polymer Free Volume and Its Connection to the Glass Transition. *Macromolecules* **2016**, *49*, 3987−4007.
(45) Buchenau, U.; Zorn, R. A Relation between Fast and Slow Motions in Glassy and Liquid Selenium. *Europhys. Lett.* **1992**, *18*, 523−528.
(46) Starr, F.; Sastry, S.; Douglas, J.; Glotzer, S. What do we learn from the local geometry of glass-forming liquids? *Phys. Rev. Lett.* **2002**, *89*, 125501.
(47) Larini, L.; Ottochian, A.; De Michele, C.; Leporini, D. Universal scaling between structural relaxation and vibrational dynamics in glass-forming liquids and polymers. *Nat. Phys.* **2008**, *4*, 42−45.
(48) Betancourt, B. A. P.; Hanakata, P. Z.; Starr, F. W.; Douglas, J. F. Quantitative relations between cooperative motion, emergent elasticity, and free volume in model glass-forming polymer materials. *Proc. Natl. Acad. Sci. U. S. A.* **2015**, *112*, 2966−2971.
(49) Simmons, D. S.; Cicerone, M. T.; Zhong, Q.; Tyagi, M.; Douglas, J. F. Generalized localization model of relaxation in glass-forming liquids. *Soft Matter* **2012**, *8*, 11455−11461.
(50) Puosi, F.; Chulkin, O.; Bernini, S.; Capaccioli, S.; Leporini, D. Thermodynamic scaling of vibrational dynamics and relaxation. *J. Chem. Phys.* **2016**, *145*, 234904.
(51) Mangalara, J. H.; Simmons, D. S. Tuning Polymer Glass Formation Behavior and Mechanical Properties with Oligomeric Diluents of Varying Stiffness. *ACS Macro Lett.* **2015**, *4*, 1134−1138.
(52) Adam, G.; Gibbs, J. H. On Temperature Dependence of Cooperative Relaxation Properties in Glass-Forming Liquids. *J. Chem. Phys.* **1965**, *43*, 139−146.
(53) Hong, L.; Novikov, V. N.; Sokolov, A. P. Is there a connection between fragility of glass forming systems and dynamic heterogeneity/cooperativity? *J. Non-Cryst. Solids* **2011**, *357*, 351−356.
(54) Casalini, R.; Capaccioli, S.; Lucchesi, M.; Rolla, P.; Corezzi, S. Pressure dependence of structural relaxation time in terms of the Adam-Gibbs model. *Phys. Rev. E: Stat. Phys., Plasmas, Fluids, Relat. Interdiscip. Top.* **2001**, *63*, 031207.
(55) Prevosto, D.; Capaccioli, S.; Lucchesi, M.; Leporini, D.; Rolla, P. Pressure and temperature dependence of structural relaxation dynamics in polymers: a thermodynamic interpretation. *J. Phys.: Condens. Matter* **2004**, *16*, 6597−6608.
(56) Schwartz, G.; Tellechea, E.; Colmenero, J.; Alegria, A. Correlation between temperature-pressure dependence of the alpha-relaxation and configurational entropy for a glass-forming polymer. *J. Non-Cryst. Solids* **2005**, *351*, 2616−2621.
(57) Schwartz, G. A.; Colmenero, J.; Alegria, A. Pressure-temperature dependence of polymer segmental dynamics. comparison

DOI: 10.1021/acs.macromol.8b01392
Macromolecules 2018, 51, 7924−7941

between the Adam-Gibbs approach and density scalings. *Macromolecules* **2006**, *39*, 3931−3938.
(58) Casalini, R.; Mohanty, U.; Roland, C. M. Thermodynamic interpretation of the scaling of the dynamics of supercooled liquids. *J. Chem. Phys.* **2006**, *125*, 014505.
(59) Casalini, R.; Roland, C. M. An equation for the description of volume and temperature dependences of the dynamics of supercooled liquids and polymer melts. *J. Non-Cryst. Solids* **2007**, *353*, 3936−3939.
(60) Roland, C.; Casalini, R. Temperature and volume effects on local segmental relaxation in poly(vinyl acetate). *Macromolecules* **2003**, *36*, 1361−1367.
(61) Heinrich, W.; Stoll, B. Dielectric Investigation of the Glass Relaxation in Polyvinyl Acetate) and Polyvinyl-Chloride) Under High Hydrostatic-Pressure. *Colloid Polym. Sci.* **1985**, *263*, 873−878.
(62) Casalini, R.; Roland, C. M. Thermodynamical scaling of the glass transition dynamics. *Phys. Rev. E* **2004**, *69*, 062501.
(63) Alba-Simionesco, C.; Cailliaux, A.; Alegria, A.; Tarjus, G. Scaling out the density dependence of the a relaxation in glass-forming polymers. *Europhys. Lett.* **2004**, *68*, 58−64.
(64) Dreyfus, C.; Le Grand, A.; Gapinski, J.; Steffen, W.; Patkowski, A. Scaling the alpha-relaxation time of supercooled fragile organic liquids. *Eur. Phys. J. B* **2004**, *42*, 309−319.
(65) Ngai, K. L.; Habasaki, J.; Prevosto, D.; Capaccioli, S.; Paluch, M. Thermodynamic scaling of alpha-relaxation time and viscosity stems from the Johari-Goldstein beta-relaxation or the primitive relaxation of the coupling model. *J. Chem. Phys.* **2012**, *137*, 034511.
(66) Dyre, J. C. Hidden Scale Invariance in Condensed Matter. *J. Phys. Chem. B* **2014**, *118*, 10007−10024.
(67) Casalini, R.; Roland, C. M. Determination of the Thermodynamic Scaling Exponent for Relaxation in Liquids from Static Ambient-Pressure Quantities. *Phys. Rev. Lett.* **2014**, *113*, 085701.
(68) Bernini, S.; Puosi, F.; Leporini, D. Thermodynamic scaling of relaxation: insights from anharmonic elasticity. *J. Phys.: Condens. Matter* **2017**, *29*, 135101.
(69) Guo, J.; Simon, S. L. Thermodynamic scaling of polymer dynamics versus T - T-g scaling. *J. Chem. Phys.* **2011**, *135*, 074901.
(70) In a more detailed treatment, the relevant position-dependent free volume value that determines a segment's dynamics could be imagined to correspond to an average over a region around the segment that extends out to some local effective range. We will not address what the range should be in this paper, as the simple method of averaging we employ here will obviate these details for the most part. These points are discussed more fully in the Appendix.
(71) Zhou, Y.; Milner, S. T. Short-Time Dynamics Reveals T-g Suppression in Simulated Polystyrene Thin Films. *Macromolecules* **2017**, *50*, 5599−5610.
(72) White, R. P.; Lipson, J. E. Thermodynamic treatment of polymer thin-film glasses. *Phys. Rev. E. Stat. Nonlin Soft Matter Phys.* **2011**, *84*, 041801.
(73) White, R. P.; Price, C. C.; Lipson, J. E. G. Effect of Interfaces on the Glass Transition of Supported and Freestanding Polymer Thin Films. *Macromolecules* **2015**, *48*, 4132−4141.
(74) Zoller, P.; Walsh, D. *Standard Pressure-Volume-Temperature Data for Polymers*; Technomic Pub Co.: Lancaster, PA, 1995.
(75) Roland, C.; Casalini, R. Temperature dependence of local segmental motion in polystyrene and its variation with molecular weight. *J. Chem. Phys.* **2003**, *119*, 1838−1842.
(76) Andersson, S.; Andersson, O. Relaxation studies of poly-(propylene glycol) under high pressure. *Macromolecules* **1998**, *31*, 2999−3006.
(77) Mckinney, J. E.; Goldstein, M. PVT Relationships for Liquid and Glassy Poly(vinyl acetate). *J. Res. Natl. Bur. Stand., Sect. A* **1974**, *78A*, 331−353.
(78) O'Reilly, J. M. Effect of Pressure on Glass Temperature and Dielectric Relaxation Time of Polyvinyl Acetate. *J. Polym. Sci.* **1962**, *57*, 429−444.
(79) Naoki, M.; Endou, H.; Matsumoto, K. Pressure Effects on Dielectric-Relaxation of Supercooled Ortho-Terphenyl. *J. Phys. Chem.* **1987**, *91*, 4169−4174.
(80) Note to be consistent with where the "bulk line" was drawn in the experimental film results in Figure 2 of ref 35 (at T = 433 K, τ = −4.03), we have correspondingly shifted the log τ_{ref} parameter from −12.60 to −12.78 and use this value for all film-related calculations that follow.
(81) Kipnusu, W. K.; Elsayed, M.; Kossack, W.; Pawlus, S.; Adrjanowicz, K.; Tress, M.; Mapesa, E. U.; Krause-Rehberg, R.; Kaminski, K.; Kremer, F. Confinement for More Space: A Larger Free Volume and Enhanced Glassy Dynamics of 2-Ethyl-1-hexanol in Nanopores. *J. Phys. Chem. Lett.* **2015**, *6*, 3708−3712.
(82) Simon, S.; Park, J.; McKenna, G. Enthalpy recovery of a glass-forming liquid constrained in a nanoporous matrix: Negative pressure effects. *Eur. Phys. J. E: Soft Matter Biol. Phys.* **2002**, *8*, 209−216.
(83) Defay, R.; Prigogine, I.; Bellemans, A.; Everett, D. H. *Surface Tension and Adsorption*; Wiley: New York, 1966.
(84) Priestley, R. D.; Cangialosi, D.; Napolitano, S. On the equivalence between the thermodynamic and dynamic measurements of the glass transition in confined polymers. *J. Non-Cryst. Solids* **2015**, *407*, 288−295.
(85) Kremer, F.; Tress, M.; Mapesa, E. U. Glassy dynamics and glass transition in nanometric layers and films: A silver lining on the horizon. *J. Non-Cryst. Solids* **2015**, *407*, 277−283.
(86) Fukao, K.; Miyamoto, Y. Glass transitions and dynamics in thin polymer films: Dielectric relaxation of thin films of polystyrene. *Phys. Rev. E: Stat. Phys., Plasmas, Fluids, Relat. Interdiscip. Top.* **2000**, *61*, 1743−1754.
(87) Lupascu, V.; Picken, S. J.; Wubbenhorst, M. Cooperative and non-cooperative dynamics in ultra-thin films of polystyrene studied by dielectric spectroscopy and capacitive dilatometry. *J. Non-Cryst. Solids* **2006**, *352*, 5594−5600.
(88) Boucher, V. M.; Cangialosi, D.; Yin, H.; Schoenhals, A.; Alegria, A.; Colmenero, J. T-g depression and invariant segmental dynamics in polystyrene thin films. *Soft Matter* **2012**, *8*, 5119−5122.
(89) Mangalara, J. H.; Mackura, M. E.; Marvin, M. D.; Simmons, D. S. The relationship between dynamic and pseudo-thermodynamic measures of the glass transition temperature in nanostructured materials. *J. Chem. Phys.* **2017**, *146*, 203316.
(90) Boucher, V. M.; Cangialosi, D.; Alegria, A.; Colmenero, J. Accounting for the thickness dependence of the T-g in supported PS films via the volume holes diffusion model. *Thermochim. Acta* **2014**, *575*, 233−237.
(91) Keddie, J. L.; Jones, R. A. L.; Cory, R. A. Size-Dependent Depression of the Glass-Transition Temperature in Polymer-Films. *Europhys. Lett.* **1994**, *27*, 59−64.
(92) Keddie, J. L.; Jones, R. A. L. Glass-Transition Behavior in Ultra-Thin Polystyrene Films. *Isr. J. Chem.* **1995**, *35*, 21−26.
(93) Koh, Y. P.; McKenna, G. B.; Simon, S. L. Calorimetric glass transition temperature and absolute heat capacity of polystyrene ultrathin films. *J. Polym. Sci., Part B: Polym. Phys.* **2006**, *44*, 3518−3527.
(94) Hanakata, P. Z.; Betancourt, B. A. P.; Douglas, J. F.; Starr, F. W. A unifying framework to quantify the effects of substrate interactions, stiffness, and roughness on the dynamics of thin supported polymer films. *J. Chem. Phys.* **2015**, *142*, 234907.
(95) Jackson, C. L.; McKenna, G. B. The Melting Behavior of Organic Materials Confined in Porous Solids. *J. Chem. Phys.* **1990**, *93*, 9002−9011.
(96) Jackson, C. L.; McKenna, G. B. Vitrification and crystallization of organic liquids confined to nanoscale pores. *Chem. Mater.* **1996**, *8*, 2128−2137.

DOI: 10.1021/acs.macromol.8b01392
Macromolecules 2018, 51, 7924−7941